KSHV-encoded vCyclin can modulate HIF1α levels to promote DNA replication in hypoxia

Rajnish Kumar Singh[1], Yonggang Pei[1], Zachary L Lamplugh[1], Kunfeng Sun[1], Yan Yuan[2], Paul Lieberman[3], Jianxin You[4], and Erle S Robertson[1*]

[1] Department of Otorhinolaryngology-Head and Neck Surgery, Perelman School of Medicine, University of Pennsylvania, Philadelphia, United States of America-19104

[2] Department of Microbiology, Levy Building, School of Dental Medicine, University of Pennsylvania, 19104

[3] Program in Gene Regulation, The Wistar Institute, 3600 Spruce Street, Philadelphia, PA 19104

[4] Department of Microbiology, Perelman School of Medicine, 3610 Hamilton Walk, University of Pennsylvania, Philadelphia, PA. 19104

***Corresponding author**

Department of Otorhinolaryngology-Head and Neck Surgery,
Department of Microbiology and The Tumor Virology Program,
Abramson Cancer Center, Perelman School of Medicine,
University of Pennsylvania,
201E Johnson Pavilion, 3610 Hamilton Walk, Philadelphia, PA, USA.
Phone: (215) 746-0114, Fax: (215) 898-9557.
E-mail: erle@pennmedicine.upenn.edu.

Abstract

The cellular adaptive response to hypoxia, mediated by high HIF1α levels includes metabolic reprogramming, restricted DNA replication and cell division. In contrast to healthy cells, the genome of cancer cells, and Kaposi's sarcoma associated herpesvirus (KSHV) infected cells maintains replication in hypoxia. We show that KSHV infection, despite promoting expression of HIF1α in normoxia, can also restricts transcriptional activity, and promoted its degradation in hypoxia. KSHV-encoded vCyclin, expressed in hypoxia, mediated HIF1a cytosolic translocation, and its degradation through a non-canonical lysosomal pathway. Attenuation of HIF1α levels by vCyclin allowed cells to bypass the block to DNA replication and cell proliferation in the hypoxia. These results demonstrated that KSHV utilizes a unique strategy to balance HIF1α levels to overcome replication arrest and induction of the oncogenic phenotype, which are dependent on the levels of oxygen in the microenvironment.

Introduction

Kaposi's sarcoma associated herpesvirus is the causative agent of Kaposi's sarcoma (KS), and is tightly linked to Primary effusion lymphoma (PEL) and Multicentric Castleman disease (MCD)[1-3]. Evidence also suggests that there is a strong association of KSHV infection with KSHV-associated inflammatory cytokine syndrome (KICS)[4, 5]. The complete nucleotide sequence of KSHV showed long unique regions (LURs) that encodes approximately 90 open reading frames[6], and many KSHV-encoded genes are now found to be homologs of cellular genes such as vCyclin, vFLIP, vGPCR, and vIRFs[7, 8]. Upon successful infection of host cells, the virus chooses to either enter a latent phase or continue towards lytic replication to generate more copies of infectious virions[9, 10]. To establish latency, the viral genome transitions through a series of epigenetic modifications that are predominantly at lysine residues on histones to minimize expression of the majority of encoded genes. Only a fraction of genes critical for latency is expressed [11, 12].

The major KSHV-encoded genes expressed in the majority of KSHV positive cancer biopsy samples include the latency associated nuclear antigen (LANA), the virus encoded homolog of human cyclin D (vCyclin), the homolog of FLICE-like inhibitory protein (vFLIP) and homologs of Interferon regulatory factors (vIRF1, vIRF2, vIRF3 and vIRF4)[13, 14]. Additionally, KSHV-positive biopsy samples are also known to have transcripts for the human homolog of the G-protein coupled receptor (vGPCR) and glycoprotein K8[13, 14]. KSHV-encoded LANA plays an essential role in maintenance of KSHV episomes within the host by tethering the KSHV DNA to the host genome[15-17]. LANA-mediated KSHV genome persistence requires its C-terminal, which binds to the KSHV DNA within its terminal repeat region while the N-terminal region of LANA binds with the host nuclear DNA[18]. LANA, in addition to tethering of the KSHV

genome regulates several cellular functions required for oncogenic transformation of infected cells. The major pathways modulated by KSHV-encoded LANA include cell cycle[19], apoptosis[20], Epithelial-Mesenchymal transition (EMT)[21, 22] and chromosome instability (CIN)[23]. Nevertheless, other KSHV-encoded latent genes also plays a major role in oncogenic transformation of infected cells. KSHV-encoded vCyclin is a homolog of host Cyclin D and is known to facilitate the G1/S transition and override contact inhibition of viral infected cells [24, 25]. Another latent antigen vFLIP is known to target the NF-kB pathway to promote oncogenesis[26-28]. Similarly, vIRFs can inhibit pro-apoptotic pathways such as those mediated by the BH3-family of proteins[29]. KSHV-encoded vGPCR, considered to be a lytic gene, was also shown to be expressed in a number of KSHV positive-tumor biopsy samples[14]. It was shown to be a bonafide oncoprotein, that regulates activities of the MAPK pathway through p38 and up-regulation of the hypoxia survival protein HIF1α[30, 31].

The latent to lytic switch of KSHV in infected cells is still not yet fully understood, but the regulation of epigenetic programs are known to be critical for this switch. Hence, the use of 12-*O*-tetradecanoylphorbol-13-acetate (TPA) and Butyric acid (BA), potent epigenetic modifiers, are effective inducers of *in-vitro* reactivation of KSHV from latently-infected cells. In addition to epigenetic modulation by TPA/BA, exposure of KSHV positive cells to hypoxia or reactive oxygen species can induce KSHV reactivation[32-36]. Independent of the method utilized for KSHV reactivation, replication competency and favorable conditions are required for initiation as well as progression of DNA replication. Among the known mediators of KSHV lytic replication, the mechanism of reactivation in response to hypoxia is still not fully understood because of its overall negative effect on replication, transcription, translation, or energy production.

Hypoxia is detrimental to aerobic cells depriving them of energy supplies due to the dramatic drop in their ability to generate ATP through oxidative phosphorylation. The adaptive response to hypoxia includes arrest of cell cycle, mainly at G1/S transition, and DNA replication due to a loss of available cellular energy stores, and the macromolecular complexes that drive these processes[37, 38]. In hypoxia, the specialized transcription factors (Hypoxia inducible factors; HIFs) are stabilized to activate transcription of stress-associated genes responsible for metabolic reprogramming, survival, angiogenesis and anti-apoptosis[39, 40]. Nevertheless, stabilization of HIF1α is known for arresting G1/S transition through regulation of the cyclin dependent kinase inhibitors p21 and p27, and other related pathways[41-43].

KSHV, like other oncogenic viruses, utilizes multiple mechanisms to maintain a high basal level of HIF1α in infected cells and infected cells are adjusted to survive with higher HIF1α levels as evident from their normal proliferation and replication potential. Paradoxically, the KSHV genome in infected cells undergoes enhanced lytic replication upon further induction of hypoxia through their ability to bypass HIF1α-mediated block to DNA replication.

The aim of the present study is to investigate the mechanism by which KSHV bypasses HIF1α-mediated repression of replication of infected cells during hypoxia. We show that, despite elevated levels of HIF1α protein, the presence of KSHV can also restrict HIF1α activity during hypoxia. Specifically, KSHV-encoded vCyclin expressed in hypoxia physically interacts with HIF1α and abrogates its transcriptional activity by mediating its degradation through a non-canonical lysosomal pathway. Knock-down of vCyclin resulted in a compromised potential of KSHV-positive cells to bypass hypoxia-mediated suppression of DNA replication, as well as their potential to proliferate in an anchorage-dependent or independent manner. These results provide new evidence to a stringently regulated control of HIF1α levels by two of its critical

104 latent antigens important for driving the oncogenic phenotype of KSHV positive cells in
105 hypoxia.

106

107

108

109

110

111

112

113

114

115

116

117

118

119

120

121

122

123

124

125

126

Results

KSHV infection restricts HIF1α transcriptional activity in hypoxia

Elevated HIF1α levels restrict DNA replication through multiple pathways. KSHV infected cells show the signature of hypoxic microenvironment with elevated levels of HIF1α, although they replicate and divide spontaneously [44]. Further, introduction of external hypoxia to KSHV positive cells is known to reactivate the virus resulting in induction of lytic replication [34, 35]. We hypothesized that despite the increased levels of HIF1α in KSHV infected cells, that the virus may negatively regulate HIF1α-mediated suppression of replication to bypass hypoxia-induced arrest of DNA replication. To investigate, we used BJAB cells containing BAC-KSHV (BJAB-KSHV cells) and the KSHV-negative BJAB cells as the isogenic cell control (with similar passage number), grown either in normoxic or hypoxic conditions. BJAB-KSHV cells were previously analyzed for other characteristics of latently infected KSHV positive cells[45]. Analysis of replication efficiency through measuring nucleotide analog incorporation in these cell lines indicated that the presence of KSHV supported sustained DNA replication in hypoxic conditions (Fig. 1A and B). As HIF1α is one of the major effectors of hypoxia and mediates repression of DNA replication in hypoxic conditions, we investigated the protein levels of HIF1α in BJAB/BJAB-KSHV cells grown in hypoxia (Fig. 1C). Western blot analysis suggested an unexpected pattern of HIF1α levels in BJAB-KSHV cells which were dramatically reduced at the 36 hr time point (Fig. 1C, lower panel). The level of HIF1α remained high in BJAB-KSHV cells as compared to BJAB cells except at this single time point of 36 hr (Fig. 1C).

To further corroborate the above findings, we examined the status of known transcriptional targets of HIF1α. The lactate dehydrogenase subunit A (LDHA), Prolyl 4-hydroxylase subunit alpha-1(P4HA1), and the Pyruvate Dehydrogenase Kinase 1 (PDK1) were examined as they are

known to be regulated by HIF1α. The results showed that the presence of KSHV had a restricted transcriptional profile for HIF1α in hypoxic conditions (Fig. 1D). For cells grown under normoxic conditions, the fold change in expression of all the studied HIF1α targets showed a significant elevated level of expression in BJAB-KSHV cells as compared to BJAB cells (2.4-fold for LDHA, 3.9-fold for P4HA1 and 1.6-fold for PDK1), suggesting a relatively high level of endogenous HIF1α in these cells (Fig.1D). Interestingly, when the expression of these targets were determined in either BJAB or BJAB-KSHV cells grown in hypoxia compared to cells from the matched experiments grown under normoxic conditions, the hypoxic BJAB-KSHV cells showed no significant increase, but a lower level of expression as compared to BJAB cells in hypoxia (Fig. 1D). Specifically, expression of LDHA, P4HA1 and PDK1 in hypoxic BJAB cells showed up-regulation of 2.5, 7.0 and 2.8-fold change, respectively, when compared to normoxic BJAB cells. However, expression of the same targets in hypoxic BJAB-KSHV cells showed up-regulation of only 0.85, 2.47 and 1.45-fold change, respectively, compared to normoxic BJAB-KSHV cells (Fig.1D). To further corroborate these results, we checked the expression of these HIF1α targets in HEK293T and HEK293T-BAC16-KSHV cells grown under normoxic or hypoxic conditions. A similar pattern of expression was also observed in these cells, suggesting that KSHV infection may restrict HIF1α transcriptional activity under hypoxic conditions (Supplementary Fig. 1C). Further validation of these results was done by infecting primary blood mononuclear cells with purified KSHV virions. PBMCs infection was carried out for 24 hours followed by incubation under normoxic or hypoxic conditions. A fraction of infected cells was used to confirm the efficiency of infection using LANA immunofluorescence (Supplementary Fig. 1A). Analysis of the HIF1α target PDK1, in infected PBMCs grown under hypoxic conditions compared to uninfected cells, showed a similar result as observed for BJAB vs BJAB-

KSHV, or HEK293T vs HEK293T-BAC-KSHV cells (Supplementary Fig. 1B). This strongly suggest a role for KSHV in the negative regulation of HIF1α on infection of human cells in hypoxic conditions.

KSHV-encoded vCyclin restricts HIF1α transcriptional activity

To confirm the repression of HIF1α by KSHV in hypoxia and rule out possibilities that the less pronounced effect of HIF1α in BJAB-KSHV during hypoxia was due to the high level of HIF1α, we transfected HEK293T cells with KSHV-encoded genes which are known to be differentially expressed under hypoxic conditions[35, 45, 46]. The expression of transfected KSHV-encoded genes was confirmed by Western blot analysis against Myc-tag (Fig. 2A). The cells were grown either in normoxic or hypoxic conditions and HIF1α transcriptional activity was checked by real-time expression of the well-established targets of HIF1α; LDHA, P4HA1, and PDK1. The results clearly showed that expression of KSHV-encoded vCyclin led to a drastic suppression in transcriptional activity of HIF1α based on the levels of its downstream targets, under both normoxic and hypoxic conditions (Fig. 2B-D and Supplementary Fig. 2). Briefly, a reduction of 2-4-fold in expression of LDHA, P4HA1, and PDK1 was observed in vCyclin expressing cells grown under hypoxic conditions as compared to the cells expressing mock or other KSHV-encoded genes including LANA and RTA grown under hypoxia (Fig. 2B-D). Furthermore, we showed that the fold change in expressions of LDHA, P4HA1 and PDK1 in vCyclin expressing cells grown under normoxic conditions were also down-regulated by 0.43, 0.83 and 0.50-fold, respectively as compared to mock transfected cells (Supplementary Fig. 2). Also, the KSHV-encoded vGPCR, a known positive regulator of HIF1α showed fold changes in expression of

LDHA, P4HA1 and PDK1 in vGPCR transfected cells to be 1.43, 1.87 and 1.9, respectively as compared to mock transfected cells (Supplementary Fig. 2).

KSHV-encoded vCyclin associates with HIF1α to mediate its cytosolic translocation

We wanted to investigate the mechanism by which vCyclin negatively regulates HIF1α transcriptional activity. We first determined whether vCyclin can associate with HIF1α in a molecular complex to inhibit its transcriptional activity. We transfected HEK293T cells with GFP-vCyclin expression plasmid to monitor their interaction. Interestingly, initial investigation for the expression of GFP-vCyclin showed a variable localization of GFP signals in both nuclear and cytosolic compartments. In the initial 24 hours, the GFP signals were predominantly localized to nuclear compartments while at a later 48 hr time, localization to the outer cytosolic compartment as punctate signals were observed (Supplementary Fig. 3). To further support this nuclear to cytosolic translocation of expressed GFP-vCyclin, we performed high resolution confocal microscopy to determine the localization of the expressed GFP-vCyclin. The results showed that vCyclin expression maintained a discrete pattern localized in the nucleus, cytoplasm or both nuclear and cytosolic compartments (Fig 3A). We hypothesized that vCyclin may associate directly with HIF1α to mediate its cytosolic translocation and hence reduce its transcriptional activity. To validate this hypothesis, we grew KSHV-positive BC3 cells in hypoxia and monitored the localization of both vCyclin and HIF1α. Colocalization of vCyclin and HIF1α in nuclear, cytosolic or both nuclear and cytosolic compartments demonstrated a potential role for vCyclin in HIF1α translocation from a prominently nuclear to cytosolic compartment (Fig. 3B). To support these data which showed the potential involvements of vCyclin in HIF1α translocation, we performed immuno-precipitation experiments using HIF1α specific antibodies. The results demonstrate that vCyclin can associate with HIF1α in molecular

complexes in KSHV cells (Fig 3C). We further validated the interaction between vCyclin and HIF1α in physiological relevant, naturally infected KSHV positive cells (BC3, BCBL1 and JSC1 cells) using immuno-precipitation assays. BJAB, a KSHV negative cell line was were also included as a control and demonstrated the complex in KSHV positive cells (Fig. 3D). Western blot analysis for HIF1α on cytosolic or nuclear fractions of HEK293T cells with and without vCyclin expression further confirmed that vCyclin-mediated HIF1α cytosolic translocation (Fig. 3E).

KSHV-encoded vCyclin down-regulates HIF1α through the lysosomal pathway

We investigated the mechanism by which KSHV-encoded vCyclin inhibited HIF1α transcriptional activity. We questioned whether the repression of HIF1α by vCyclin was due to suppression of its transcriptional activity or was it due to changes at the level of the protein, as we observed reduced expression of HIF1α in KSHV positive cells after 36 hours post-hypoxia induction (Fig. 1C). We transfected HEK293T cells with an expression plasmid encoding vCyclin followed by western blot analysis for HIF1α. To rule out involvement of other KSHV antigens that was previously shown to be associated with HIF1α, we transfected HEK293T cells with KSHV-encoded LANA, vGPCR, vFLIP and RTA plasmids (Fig. 4A). Expression of KSHV-encoded antigens was previously confirmed by western blots against the fused epitope tag or the viral antigen (Fig 2A), followed by monitoring expression of HIF1α (Fig. 4A). The results demonstrated that expression of vCyclin down-regulated HIF1α protein levels by greater than 50 percent (Fig. 4A). To further corroborate these findings, we transfected HEK293T cells with increasing amounts of expression plasmids encoding vCyclin followed by western blot to monitor HIF1α expression. As expected, HIF1α expression levels were continually decreased

with increasing amounts of vCyclin (Fig. 4B). These results were supported using another cell line Saos-2 (Supplementary Fig. 4A-B). To further study the detailed mechanism of vCyclin mediated degradation of HIF1α, we generated stable cells with mock or GFP-vCyclin expressing plasmids. Interestingly, we observed that in contrast to mock transfected cells, signals for vCyclin as monitored by GFP gradually decreased and eventually were lost even under selection (Fig. 4C). The cytosolic translocation of expressed vCyclin, its elimination over time in cells, and its interaction with HIF1α led us to hypothesize that vCyclin may mediate degradation of HIF1α through the lysosomal pathway. Therefore, we treated cells expressing vCyclin with a lysosomal inhibitor (Chloroquine) with increasing concentration. We also treated these cells with the proteosomal inhibitor (MG132) to rule out proteosomal degradation[47]. The results clearly showed that treatment of cells expressing vCyclin with the proteosomal inhibitor MG132 failed to protect degradation of HIF1α.However, treatment of these cells with the lysosomal inhibitor Chloroquine protected HIF1α from vCyclin-mediated degradation (Fig.4D). The results were also similar in the Saos-2 cell line (Supplementary Fig. 4C) These results clearly demonstrated that KSHV-encoded vCyclin is involved in degradation of HIF1α through the lysosomal pathway. To further corroborate these findings, we investigated the subcellular localization of HIF1α in cells expressing Myc-tagged KSHV-encoded vCyclin, especially with respect to its lysosomal localization. Interestingly, we observed that HIF1α localized to the nucleus as well as lysosomal compartments, as seen in the representative image of HIF1α in vCyclin expressing cells (Fig. 4E).

To understand the relevance of vCyclin-mediated HIF1α attenuation, we further investigated the details of vCyclin expression under hypoxic conditions. We recently observed that KSHV-encoded vCyclin transcripts were up-regulated in KSHV positive BC3 cells grown under

hypoxic conditions. We further corroborated these findings by using two KSHV-positive cells lines, BCBL1 and JSC1[45]. We treated these cells with the chemical mimetic of hypoxia, $CoCl_2$ for 8 hours to prevent VHL ubiquitin-ligase mediated degradation in normoxia and stabilization of HIF1α in those cells[48]. HIF1α levels were monitored by western blot using HIF1α specific antibodies (Supplementary Fig. 5A). The real-time PCR for vCyclin transcripts in these cells confirmed that hypoxia positively upregulated expression of KSHV-encoded vCyclin (Supplementary Fig. 5B).

We further investigated the detailed mechanism by which HIF1α upregulated vCyclin expression and its negative feedback on HIF1α regulation. The promoter region of vCyclin was therefore analyzed for the presence of functional hypoxia responsive elements (HREs). A schematic for the KSHV latent gene locus (LANA, vCyclin and vFLIP) is shown (Supplementary Fig. 5C). As the HREs within LTc or LTi promoter region are already studied and these HREs are common for all the three latent genes (LANA, vCyclin and vFLIP) [46], here we focused on the HREs mainly in the promoter region downstream to them and specific for ORF71 and ORF72 (LTd) [46].

The *in-silico* analysis of the vCyclin promoter (Ltd promoter) revealed the presence of four distinct HREs (Supplementary Fig. 5C). To determine if these HREs are directly under the transcriptional regulation of HIF1α, we cloned these HREs into the luciferase reporter plasmid vector. Co-transfection of HIF1α with the promoter constructs was performed to determine which if any of the HREs within the Ltd promoter was predominantly responsible for vCyclin transactivation. The luciferase-based analysis suggested that the 1st HRE is the most responsive towards elevated HIF1α (Supplementary Fig. 5D). These results suggested a feedback regulation of HIF1α expression through KSHV-encoded vCyclin.

KSHV infection rescues HIF1α-mediated negative regulation of DNA replication.

In hypoxia, HIF-1α is known to bind with Cdc6, a crucial protein required for loading cellular helicases (MCMs) onto DNA to initiate DNA replication[49]. This also explains HIF1α-mediated repression of DNA replication in hypoxia. We hypothesized that the presence of KSHV could abrogate hypoxia-mediated negative regulation of DNA replication through vCyclin-dependent HIF1α degradation. For this, we wanted to investigate the HIF1α enrichment on KSHV genome using Chromatin Immunoprecipitation (ChIP) sequencing. As the complete degradation of HIF1α through expression of vCyclin did not represent a physiological condition for KSHV-infected cells growing under hypoxic conditions, we infected PBMCs with KSHV followed by growing the mock or infected cells in normoxic or hypoxic conditions. KSHV infection was monitored by LANA immuno-fluorescence and was confirmed by LANA western blot (Fig. 5A and B). We also included naturally infected KSHV positive BC3 cells for ChIP sequencing (Fig. 5C). Chromatin immuno-precipitation (ChIP) was performed using HIF1α antibody followed by ChIP-sequencing. The ChIP-sequencing results for enrichment of HIF1α on the KSHV genome showed that even in the presence of KSHV, either in infected PBMCs or BC3, there is an almost 4-fold high enrichment of HIF1α on KSHV genome in hypoxia (Fig. 5D and E). Interestingly, the HIF1α enriched regions were mostly located at regions away from the origin of lytic replication (located between K4.2 and K5, and between K12 and ORF71) [50] (Fig. 5D, E and Supplementary Table 2-5). This suggests that during the period examined for hypoxic induction, there was likely no suppression of DNA replication through direct binding of HIF1α to the OriLyt region. Moreover, high enrichment of HIF1α on KSHV genome can be an indicative of enhanced transcription of KSHV-encoded lytic genes required for KSHV

reactivation (Fig. 5D and E). Further, details of HIF1α enriched regions on the KSHV genome in normoxic or hypoxic conditions are provided in Supplementary Tables 2-5.

Knock-down of vCyclin in KSHV positive cells attenuated KSHV-mediated bypass of hypoxia induced DNA replication and proliferation.

We investigated the effects of knocking down KSHV-encoded vCyclin on DNA replication as well as proliferation of KSHV positive cells grown under hypoxic conditions. We generated lentivirus mediated vCyclin knock-down in KSHV positive BC3 cells (Fig. 6A). The knock down of vCyclin was confirmed at the transcript level by real time PCR using cDNA from ShControl or ShvCyclin transduced BC3 cells. A four-fold or greater down-regulation of vCyclin was seen at the transcript level (Fig. 6B). The BC3 ShControl or ShvCyclin cells were grown under normoxic conditions or in 1%O_2 to induce hypoxic conditions, and DNA replication and cell growth were examined under hypoxic conditions. The effects of hypoxia-mediated repression of replication in vCyclin knockdown, KSHV positive BC3 cells was investigated by copy number calculation of KSHV genome in these cells grown under normoxia or hypoxia. As compared to BC3-ShControl, BC3-ShvCyclin cells showed an adverse effect on KSHV replication as evident from more than 10-fold less KSHV copy number in hypoxia (Fig. 6C). The results demonstrated the compromised replication potential of KSHV positive cells when vCyclin was knocked down. Interestingly, knock-down of vCyclin adversely affected replication even under normoxic conditions (Fig. 6C). We further validated these results at the level of single molecules of KSHV genome using single molecule analysis of replicated DNA (SMARD). In brief, ShControl, BC3-ShvCyclinBC3 cells were grown under hypoxia for 24

hours followed by pulsing of these cells by nucleotide analogs to study their incorporation into replicating KSHV genomes. Pulsed cells were molded in agarose plugs followed by Proteinase K digestion of cellular proteins. The agarose embedded DNA was digested with Pme1 restriction enzyme to linearize the KSHV genome. The Pme1 digested DNA was then fractionated on pulse field gel electrophoresis followed by Southern blot against KSHV DNA to define and excise the agarose slices containing KSHV genome (Fig. 6D). The identified slice was melted and agarose was digested with Gelase followed by stretching the DNA on silanized slides. The linearized KSHV genomes on the slides were visualized with three KSHV specific probes (KSHV co-ordinates: 26937-33194(6kb); KSHV co-ordinates: 36883-47193 [(10kb) and KSHV co-ordinates: 85820-100784(15kb)][51]. The incorporated nucleotides in replicated DNA was probed with Alexa-conjugated secondary antibodies against the primary antibodies of IdU and CldU. A KSHV molecule with incorporated nucleotide analogs represented a genome that was replicated. The analysis of SMARD clearly demonstrated that knock down of vCyclin suppressed KSHV replication by more than 10-fold in hypoxia (Fig. 6E and F).

We then investigated the potential of vCyclin knock down of KSHV positive cells on anchorage dependent and independent growth. ShControl or ShvCyclin of HEK293T-BAC16-KSHV cells were used to generate anchorage dependent colonies while ShControl or ShvCyclin of BC3 cells were used to generate anchorage independent colonies in soft agar. Both types of colonies were challenged to growth in hypoxia for 72 hours followed by staining and visualization through trypan blue staining. The results showed that ShvCyclin cells were highly compromised for both anchorage dependent, and independent growth as evident from the size and number of colonies (Fig. 6G).

Discussion

Hypoxia represents a detrimental stress to aerobic cells and is an established physiological character of cancer as well as oncogenic virus infected cells[52, 53]. The hypoxic cells, not only need a large scale reprogramming of cellular pathways for survival, but also poses a major challenge for patients undergoing chemotherapy and radiation therapy[54]. The well-known factors responsible for reprogramming of cellular pathways under hypoxic conditions include the hypoxia inducible factors (HIFs) which possess broad transcriptional capacity for cells grown in hypoxia[40]. HIF1α is considered rate limiting protein based on its stabilization, specifically under hypoxic conditions[40]. When stabilized, HIF1α transactivates genes involved in, but not limited to those associated with glucose transport (GLUTs), glycolysis (HK1, HK2, ENO1, GPI, and LDHA), angiogenesis (VEGF, ENG, and LRP1), growth & survival (Cyclin G2, TGF-b, EPO, and NOS), and invasion and metastasis (KRTs, MMP2, UPAR, AMF, and PAI1)[39, 40, 55]. Based on these broad roles of HIF1α in growth and survival, the protein is often considered an oncogenic protein[56]. Under favorable normoxic conditions, the protein levels of HIF1α is tightly regulated through its proteosomal degradation by the tumor suppressor protein VHL or lysosomal degradation mediated by cyclin dependent kinase 2 (CDK2)[57-59].

KSHV, like other oncogenic viruses, utilizes multiple mechanisms to up-regulate and stabilize HIF1α[44, 60-63]. Elevated HIF1α in KSHV infected cells is known to modulate expression of

key oncogenes encoded by KSHV in an autocrine manner, in addition to transactivation of cellular genes responsible for survival, growth, proliferation, angiogenesis and metabolic reprogramming[64-68]. KSHV-encoded vGPCR effects on the p38/MAPK pathway, and EC5S-mediated ubiquitination of the tumor suppressor VHL by KSHV-encoded LANA are extensively studied pathways which shows upregulated expression of HIF1α in KSHV infected cells [69, 70]. HIF1α also upregulates vGPCR in a cyclic manner to maintain continued elevated levels of HIF1α, and targeting HIF1α in KSHV infected cells has been proposed as a potential therapeutic strategy against KSHV-mediated oncogenesis[45, 71]. It is noteworthy that hypoxia or elevated HIF1α levels induces arrest of cell cycle and DNA replication to minimize energy utilization as well as the macromolecular demands on cells, and this arrest is crucial for survival until favorable conditions return. Nevertheless, HIF1α-mediated inhibition of cell cycle progression and DNA replication depends on both transcriptional, as well as non-transcriptional activity of HIF1α[41-43, 49, 72-74].

Paradoxically, in contrast to healthy cells with arrested cell cycle and DNA replication, KSHV infected cells not only divide and replicate in hypoxia, but is induced to productive (lytic) replication[34, 35, 41, 43]. We investigated the mechanism behind bypassing hypoxia-induced replication arrest in KSHV positive cells. However, KSHV studies have been somewhat hindered by a lack of isogenic KSHV negative control cell lines. Infection based studies also include constraints with variable expression of KSHV-encoded genes, as well as initial epigenetic reprogramming of the KSHV genome upon entry into infected cells. In the present study we used KSHV negative BJAB cells matched with its counterpart BJAB-KSHV cells (BJAB cells stably transfected with BAC-KSHV)[75]. These cell lines were characterized for their isogenic background through short tandem repeats (STR) profiling[45]. Additionally, BJAB-KSHV cells

were checked for typical characters of latently infected KSHV-positive cells and a similar passage number of cells were used in this study to rule out any further constraints[45]. Replication rate analysis of these two cell lines grown under hypoxic conditions clearly demonstrated that the presence of KSHV helped in bypassing hypoxia-mediated replication arrest despite having a higher level of HIF1α in normoxia and hypoxia. The higher levels of HIF1α appeared to be aligned with its transcriptional activity where these cells have significantly higher levels of HIF1α targeted downstream transcripts such as PDK1, LDHA and P4HA. Interestingly, the introduction of hypoxia to these cells through growth in low oxygen resulted in significantly less upregulation of these HIF1α targets in BJAB-KSHV cells compared to matched KSHV negative BJAB cells. This result suggested that BJAB-KSHV cells were adjusted for growth with higher levels of HIF1α and show the same growth pattern as KSHV negative BJAB cells in normoxic conditions. However, the presence of KSHV negatively regulated the transcriptional activity of HIF1α in hypoxic conditions to provide an advantage for cell proliferation compared to KSHV negative BJAB cells. A similar result was seen in PBMCs infected with mock or rKSHV and further confirms the role of the virus in DNA replication of infected cells grown under hypoxic conditions. In addition, it provides new insights into a role for KSHV latent antigens, which was also expressed upon infection as well as under hypoxic conditions, with a major role in this transition.

The KSHV-encoded LANA, RTA, vGPCR, vCyclin and vFLIP are well-established antigens expressed during latency, initial infection or under hypoxia induction. Expression of these antigens individually when compared to mock revealed that vCyclin can efficiently down-regulate the transcriptional activity of HIF1α. Additionally, expression of GFP-tagged vCyclin in cells showed a variable localization within either nuclear, cytosolic or both nuclear and cytosolic

compartments. Further, long term expression of vCyclin was unsuccessful after selection in culture. These results provide new insights into a role for collaboration of vCyclin with HIF1α in mediating its cytosolic translocation, and the degradation of both vCyclin and HIF1α within the lysosomal compartment. Immunoprecipitation of HIF1α with vCyclin, the co-localization of both vCyclin and HIF1α to the lysosomal compartment in vCyclin expressing cells, and their degradation as well as their protection from degradation in cells treated with chloroquine, the lysosomal inhibitor, clearly demonstrated a role for vCyclin in regulation of lysosomal degradation of HIF1α in KSHV positive cells in hypoxia. It is important to note that, in KSHV positive cells, HIF1α itself upregulated expression of vCyclin through HREs transactivation forming a negative feedback control (Fig. 7).

ChIP-Sequencing results of KSHV infected cells grown under normoxic or hypoxic conditions to define the transcriptional activity or repression of replication due to HIF1α in these cells under physiologically relevant conditions showed significantly high reads across the KSHV genome in hypoxia, especially near the latency locus. Further analysis of the ChIP-seq results provided ample information about the regulation of HIF1α transcriptional activity on the KSHV genome. Further, it provides an explanation for how the KSHV lytic origin of replication was derepressed by HIF1α-mediated blockage of replication (Green highlighted area at the bottom of the histogram) (Fig. 5). Overall, the present studies clearly demonstrated that KSHV-encoded vCyclin attenuates HIF1α signaling in a negative feedback loop to create a favorable environment where DNA replication is permitted. The work also explores a new area of investigation as to the role of another oncogenic viral encoded antigen in driving DNA replication in hypoxia. It also extends our knowledge as to the stringent regulation of HIF1α required for KSHV genome replication and cell proliferation by three KSHV-encoded antigens

448 and explores their complementary roles for viral genome persistence and survival of the infected
449 cells in the hypoxic microenvironment.
450
451
452
453
454
455
456 **Materials and methods**
457 **Ethics statement**
458 University Pennsylvania Immunology Core (HIC) provided human peripheral blood
459 mononuclear cells (PBMC) from different unidentified and healthy donors with written,
460 informed consent. All the procedures were approved by the Institutional Review Board (IRB)
461 and conducted according to the declarations of Helsinki protocols.
462
463 **Cell lines, Plasmid vectors, transfection and lentivirus transduction**
464 BJAB, BJAB-KSHV, BC3, BCBL1, JSC1 and PBMCs were maintained in RPMI medium
465 supplemented with 10% bovine growth serum (BGS) and antibiotics. HEK293T cells were
466 maintained in DMEM medium with 5% BGS and antibiotics. Constructs for Myc-tagged LANA
467 and Myc-tagged RTA constructs were described earlier[16]. KSHV-encoded vCyclin and vFLIP
468 were amplified by PCR, and ligated to the EcoR1/Xho1 restriction site of the pA3M vector.
469 KSHV-encoded vGPCR was amplified by PCR from pCEFL-vGPCR plasmid vector (a gift from
470 Enrique A Mesri, University of Miami) and sub-cloned into the EcoR1/Xho1 restriction site of

pA3M plasmid vector. GFP-tagged-vCyclin and constructs were generated by PCR amplification and cloned into the pLVX-Ac-GFP vector. Transfections were carried out using jetPRIME reagent (Polyplus Transfection Inc., New York, NY) or through Calcium-phosphate based methods. ShRNA targeting KSHV-encoded vCyclin was generated in pGIPZ vector. For production of lentivirus, pGIPZ clones along with packaging and helper plasmids were transfected into HEK293T cells as described earlier[45]. Lentivirus transduction was performed in a total volume of 1ml in the presence of 20 µg/ml Polybrene. Unless otherwise stated, all cultures were incubated at 37°C in a humidified environment with 5% CO_2. For hypoxic induction, cells were grown in the presence of 1% O_2 in a humidified chamber. The LTd promoter and deletion constructs for various hypoxia responsive elements (HREs) namely, HRE1, HRE2, HRE3 and HRE4 were cloned into the luciferase reporter plasmid pGL3-basic vector (Promega Corporation, Madison, WI).

KSHV virion purification and infection of PBMC

KSHV-positive BC3 cells were used for production of virus through reactivation and purification of KSHV for infections. Briefly, cells were grown in culture medium containing TPA and butyric acid at a final concentration of 20 ng/ml and 3mM, respectively for 4-5 days. Cells and the medium were collected and centrifuged at 3,000rpm for 30 minutes to collect supernatant. The cell pellet was resuspended in 1X PBS and the cells were ruptured by freeze thaw, followed by centrifugation at 3000rpm for 30 minutes. The supernatant were collected and pooled followed by filtration through 0.45 µm filter. The viruses were concentrated by ultracentrifugation at 23,500 rpm at 4°C for 2 hours. The KSHV genomic region (36883-47193)[51] cloned in pBS-puro plasmid was used to generate a standard curve for copy number

494 calculation of the purified virus. PBMCs were infected with purified KSHV virions at a
495 multiplicity of infection of 10 in a total volume of 1ml in the presence of 20 µg/ml Polybrene.
496 The rate of infection was monitored by immuno-fluorescence to detect LANA expression.
497
498 **Western blotting and Immunoprecipitation**
499 Primary antibody against Myc-tag was purified from 9E10 hybridoma (a gift from Dr. Richard
500 Longnecker, Northwestern University). Antibodies for GFP and GAPDH were obtained from
501 Santa Cruz Biotechnology (Dallas, TX). Histone H4 antibodies were procured from Millipore
502 (Burlington, MA). Antibodies used against LANA was purified hybridoma hybridoma (a gift
503 from Dr. Ke Lan, Key State Virology Laboratory, Wuhan, China). HIF1α antibodies were
504 obtained from Novus Biologicals (Centennial, CO). vCyclin antibodies were obtained from
505 Abcam (Cambridge, MA). Cells were lysed with radio-immunoprecipitation (RIPA) buffer (50
506 mM Tris; pH 7.6, 150 mM NaCl, 2 mM EDTA, 1% Nonidet P-40) supplemented with protease
507 inhibitors (Aprotinin [1 g/ml], Leupeptin [1 g/ml]and Pepstatin [1 g/ml] and
508 phenylmethylsulfonyl fluoride (PMSF)[1 mM]). Equal amounts of protein were fractionated on
509 SDS-PAGE followed by transfer to nitrocellulose membrane. Protein transfer was monitored
510 through Ponceau staining and the membrane was washed with TBST followed by blocking in 5%
511 skimmed milk. Primary antibody incubation was performed at 4°C overnight with gentle
512 shaking. Infrared conjugated secondary antibodies were used to probe and capture protein levels
513 using an Odyssey scanner (LiCor Inc. Lincoln, NE). For immuno-precipitation, transfected cells
514 were lysed in RIPA buffer and proteins were pre-cleared with protein A/G agarose beads. The
515 pre-cleared lysates were incubated with the specific antibodies overnight at 4°C with gentle
516 shaking. Protein A/G agarose beads slurry were used to collect the immune complexes. The

beads were washed 3 times with 1X phosphate buffer saline followed by resuspension in equal volumes of 2X SDS loading dye. Approximately, 5% sample was used as input control.

Fractionation of nuclear and cytoplasm proteins

Transfected cells were harvested by scraping on ice-cold PBS and collected by centrifugation at 1,000 rpm for 5 minutes. The supernatants were discarded and the cell pellet were resuspended in hypotonic lysis buffer (20 mM HEPES-K^+ [pH 7.5], 10 mM KCl, 2 mM $MgCl_2$, 1 mM EDTA, 1 mM EGTA, 0.5M dithiothreitol) in the presence of protease inhibitors (1mMphenylmethylsulfonyl fluoride, aprotinin [1g/ml], leupeptin [1g/ml]and pepstatin [1g/ml], 10µg of phenanthroline/ml, 16µg of benzamidine/ml) for 20 minutes. Samples were passed through 27-gauge needle 10 times before nuclei were pelleted by centrifugation at 3,000 rpm for 5 minutes. The Cytosolic supernatant was collected and centrifuged at 15,000 rpm for 15 minutes at 4°C to obtain the clear lysate. The nuclear pellet were resuspended in lysis buffer for a second time and passed through 25-gauge needle for 10 times followed by centrifugation at 3,000 rpm for 10 minutes. Nuclear pellet was resuspended in 1X TBS, 0.1% SDS. Genomic viscosity was removed by sonication of the samples using QSONICA sonicator (Newtown, CT).

Quantitative real-time PCR

Total RNA from cells was extracted through standard phenol chloroform extraction using Trizol. RNA concentration and quality were measured using a biophotometer and on multimode spot reader using a Cytation^{TM} 5 (BioTek Inc. Winooski, VT). Total RNA from different samples were used to synthesize cDNA using Superscript II reverse transcription kit (Invitrogen, Inc., Carlsbad, CA). 1µl of 10X dilution of cDNA was used per reaction for real-time quantitative

PCR in a total volume of 10 µl using SYBR green reagent. A melting curve analysis was performed to verify the specificity of the amplified products. The relative fold change in expression were calculated by the delta delta threshold cycle method and each sample were measured in triplicates. The sequences of primers used for real-time PCR are given in Table S1.

Immunofluorescence

Cells on a glass coverslip were fixed using 4% PFA for 20 min at room temperature followed by washing in 1X PBS. A combined blocking and permeabilization of cells were performed for 1 hour in 1X PBS containing 0.1% Triton X-100 with 5% serum from the species used to generate secondary antibody. Primary antibodies were diluted in 1X PBS/0.1% Triton X-100 and incubated overnight at 4°C followed by three times washing in 1X PBS. Secondary antibodies were diluted in 1X PBS at a concentration suggested by manufacturer and incubated at room temperature for 1 hour followed by three times wash in 1X PBS. Nuclei were stained using DAPI at a final concentration of 1µM for 20 minutes at room temperature followed by washing in 1X PBS. The slides were mounted using anti-fade reagent and sealed with colorless nail polish. The slides were kept at -20°C until use for capturing images with an Olympus confocal microscope (Olympus Corp., Tokyo, Japan).

Chloroquine and MG132 Treatment, and Lysotracker staining

The cytotoxic effect of chloroquine and MG132 was determined based on previously published studies[76, 77]. Chloroquine was used at a concentration of 50 µM, and 5µM was used as a maximum concentration of MG132 to treat cells. 24 hours post-transfection, the culture medium was replaced with fresh medium containing either Chloroquine or MG132. For Chloroquine

563 treatment, a wide range of concentration (0, 6.25, 12.5, 25 and 50µM) was used for 24 hours.
564 Similarly, for MG132, the range of concentration used was 0.625, 1.25, 2.5 and 5 µM and the
565 treatment time was for 24 hours. Lysotracker staining was performed on live cells grown on
566 cover slip at 75nM final concentration of Lysotracker™ Deep red (ThermoFisher Scientific
567 Inc., Grand Island, NY)
568
569 **Colony formation and soft agar assays**
570 For colony formation and soft agar assays, KSHV positive BC3 cells were transduced with
571 lentivirus coding either ShControl or ShvCyclin. The transduced cells were selected under
572 puromycin for 3 weeks. 100% stably transduced (GFP positive) cells were used for colony
573 formation and soft agar assay. 10 million HEK293T-KSHV cells were transfected with pGIPZ-
574 shCon, sh-HIF1α or ShvCyclin plasmids by electroporation and seeded in 10cm dishes.
575 Transfected cells were grown in DMEM containing puromycin at 0.5µg/ml concentration. After
576 selecting the cells for up to 2-weeks, selected cells were fixed with 4% formaldehyde and stained
577 with 0.1% Crystal Violet solution (Sigma-Aldrich Corp., St. Louis, MO). The area of the
578 colonies was calculated by using Image J software (Adobe Inc., San Jose, CA). The data shown
579 here represents the average of three independent experiments.
580
581 **Luciferase reporter assays**
582 Full length LTd promoter or deletion construct for different HREs were cloned into pGL3 basic
583 vector between Mlu1 and Xho1 restriction sites through PCR based method. HEK293T cells
584 were transfected with either full length LTd promoter or deletion constructs of HREs. The cells
585 were harvested at 48 h post-transfection and subsequently washed once with PBS, followed by

lysis with 200 µl of reporter lysis buffer (Promega, Inc. Madison, WI). 40 µl of the total protein lysate was mixed with 25 µl of luciferase assay reagent. Luminescence was measured on a Cytation^{TM} 5 multimode reader (BioTek, Inc. Winooski, VT). Relative luciferase activity was expressed as fold activation relative to that of the reporter construct alone. The results shown represent assays performed in triplicate. The sequences of primers used to clone full length LTd promoter or various HREs deletion constructs are given in Table S1.

Statistical analysis

All experiments were performed in replicates of three. The results were presented as means ± standard deviations (SDs). The data was considered statistically significant when the p-value was <0.05 using the Student's t-test.

Single molecule analysis of replicated DNA (SMARD)

Single molecule analysis of replicated DNA of KSHV was performed as described earlier [51]. In brief, cells pulsed with nucleotide analog (Chlorouridine, CldU, 10 µM and Iodouridine, IdU, 10 µM) were mixed with InCert agarose to make plugs. Plugs were digested with proteinase K followed by linearizing KSHV genome by digesting with Pme1 restriction enzyme. Plugs were run on pulse field gel electrophoresis (PFGE). A portion of gels were used to perform Southern blot to locate and excise the gel regions enriched with KSHV genome. Gel slices were digested with agarose and DNA was stretched on silanized glass slides. KSHV genome was probed with

608 KSHV specific hybridization probes. Incorporation of CldU and IdU was visualized after
609 probing with specific antibodies.
610
611 **ChIP sequencing**
612 Cells were grown in either normoxia or 1% O_2 induced hypoxia. Cells were crosslinked by
613 adding formaldehyde to a final concentration of 1% at room temperature. Crosslinking was
614 stopped by adding glycine with shaking. Cells were collected by centrifugation and washed three
615 times before resuspending in PBS. Cell pellets were resuspended in cell lysis buffer (5mM
616 PIPES pH8.0/85mM KCl/0.5% NP-40) containing protease inhibitors (1µg/ml Aprotinin, 1µg/ml
617 Leupeptin, 1µ/ml Pepstatin and 1mM PMSF). Cells were incubated on ice and homogenized
618 with several strokes using a douncer. Nuclei were collected by centrifugation and lysed by
619 adding nuclear lysis buffer (50 mM Tris, Ph8.0/10 mM EDTA/1% SDS containing same
620 protease inhibitors). After nuclear lysis, chromatin were fragmented to an average size of 300-
621 400 bp with a Branson sonifier 250 with a microtip and cooling on ice. Cell debris was cleared
622 by centrifugation and ChIP library preparation and adaptor ligation was performed using
623 Illumina ChIP-sequencing sample preparation kit according to manufacturer protocol. ChIP-
624 sequencing was performed at University of Washington sequencing core (St. Louis, MO). The
625 data was analyzed using CLC Bio software (Qiagen Inc. Germantown, MD).
626

Acknowledgements

We are grateful to Enrique A Mesri (Miller school of Medicine, University of Miami), for kindly providing pCEFL-vGPCR construct. This work was supported by the National Cancer Institute at the National Institutes of Health under award numbers P30-CA016520, P01-CA174439, U54-CA190158, R01-CA171979 and R01-CA244074 (to E.S.R.). The funders had no role in study design, data collection, and analysis, decision to publish, or preparation of the manuscript.

Competing interests

The authors declare no financial or non-financial competing interest exists.

650 **Figure Legends**

651 **Fig. 1:** KSHV infection restricts HIF1α activity to promote DNA replication. (A) Representative
652 image of YOYO-1 staining of stretched DNA and nucleotide analog incorporation in BJAB and
653 BJAB-KSHV cells grown under normoxic or hypoxic conditions (B) quantitation of nucleotide
654 analog incorporation in BJAB and BJAB-KSHV cells grown under normoxic or hypoxic
655 conditions. Cells pulsed with IdU were probed with anti-IdU antibodies and the relative
656 incorporation was measured using a FACS machine. (C) Representative HIF1α western blot
657 analysis in BJAB and BJAB-KSHV cells grown under normoxia or hypoxic conditions. The cells
658 were either grown under normoxic or hypoxic conditions for the indicated time period. Equal
659 amounts of protein were used to detect HIF1α from the lysate of these cells. GAPDH western
660 Blot served as the loading control. (D) Real-time PCR analysis for the transcriptional activity of
661 HIF1α in BJAB and BJAB-KSHV cells grown under normoxic or hypoxic conditions. The cells
662 were grown under normoxic or hypoxic conditions followed by total RNA isolation and cDNA
663 synthesis. Equal amounts of cDNA were used for expression analysis of HIF1α targets (LDHA,
664 PDK1 and P4HA1) by real-time PCR. The experiment was performed in triplicate. The error bar
665 represents standard error from the mean. A p-value of <0.05 (*) was taken into consideration for
666 statistical significance.

667

668 **Fig. 2:** KSHV-encoded vCyclin restricts HIF1α transcriptional activity. (A) Expression of
669 KSHV-encoded antigens. Mock, myc-tagged vCyclin, myc-tagged vGPCR, myc-tagged LANA,
670 myc-tagged RTA or myc-tagged vFLIP plasmids were transfected into HEK293T cells followed
671 by western blot analysis using anti-myc antibody. (B-D) Real-time PCR expression analysis of
672 HIF1α targets LDHA, P4HA1 and PDK1 in HEK293T cells transfected with Mock, LANA,

673 RTA, vFLIP, vCyclin or vGPCR plasmids and grown under hypoxic conditions compared to
674 Mock transfection grown under normoxic or hypoxic conditions. 24 hours post transfection, cells
675 were grown for another 24 hours in hypoxic conditions. Total RNA was isolated from
676 transfected cells followed by synthesis of cDNA using 2 µg of the total RNA. Equal cDNA was
677 used for quantitative real-time PCR. GAPDH was used as the endogenous control. The
678 experiments were done in triplicate. The error bar represents standard error from the mean. A p-
679 value of <0.05 (*) was taken into consideration for statistical significance.
680
681 **Fig. 3:** KSHV-encoded vCyclin physically interacts with HIF1α and mediates its cytosolic
682 translocation. (A) HEK293T cells were transfectetd with GFP-vCyclin encoding plasmids. The
683 transfected cell were analyzed for cellular localization of expressed proteins through GFP
684 fluorescence with reference to nucleus (DAPI signals). The GFP signals showed a clear
685 distribution to the nuclear, cytosolic or nucleo-cytosolic compartments. (B) Microscopic
686 investigation of HIF1α sub-cellular localization in vCyclin expressing KSHV-positive BC3 cells
687 grown under hypoxic conditions. Cells were seeded on coverslips. The coverslip-attached cells
688 were fixed, permealized, blocked and probed with vCyclin and HIF1α antibodies. Nuclei were
689 stained with DAPI. Both vCyclin and HIF1α showed a clear distribution to the nuclear, cytosolic
690 or nucleo-cytosolic compartments. (C) Immuno-precipitation of vCyclin with HIF1α in
691 HEK293T cells. GFP-vCyclin transfected cells were lysed in radio-immunoprecipiation buffer
692 and protein were pre-cleared with protein agarose A/G beads followed by overnight immuno-
693 precipitation with GFP antibody. The immune complexes were collected with protein agarose
694 A/G bead slurry. The beads were washed with PBS and were resuspended in 2X SDS loading
695 dye. 1/3rd of the immuno-precipitated complex was run on 10% SDS PAGE against 5 % input or

696 IgG control sample and probed with HIF1α or GFP (for vCyclin) antibodies. (D) HIF1α
697 immuno-precipitation using vCyclin antibodies in KSHV positive BC3, BCBL1 and JSC1 cells.
698 KSHV negative BJAB cells were used as a negative control. (E) Western blot analysis for
699 nuclear, cytosolic or nucleo-cytosolic localization of HIF1α in vCyclin expressing cells. The
700 transfected cells were lysed to separate into nuclear or cytosolic fraction as described in the
701 materials and methods section. The nuclear or cytosolic fractions were checked for localization
702 of HIF1α. GAPDH and Histone H4 served as loading controls for cytosolic and nuclear fraction
703 respectively. Asterisk represents non-specific bands.
704
705 **Fig. 4:** KSHV-encoded vCyclin degrades HIF1α in a dose dependent manner through the
706 lysosomal pathway. (A) Mock or KSHV-encoded vCyclin, LANA, RTA, vGPCR and vFLIP
707 were transfected into HEK293T cells followed by investigating HIF1α levels. Equal amounts of
708 protein were used to probe HIF1α levels. GAPDH was used as the loading control (B) HIF1α,
709 GFP-vCyclin and GAPDH western blots of cells transfected with gradually increasing amounts
710 of GFP-vCyclin. GFP western blot represents GFP-vCyclin. GAPDH was used as the loading
711 control. (C) Representative image for generation of mock or GFP-vCyclin stable cell lines (D)
712 HIF1α western blot analysis of HEK293T cells transfected with GFP-vCyclin and treated with
713 increasing amounts of lysosomal inihibitor (Chloroquine; 0, 6.25, 12.5, 25 and 50μM) or
714 proteosomal inhibitor (MG132; 1.25, 2.5, 5 and 10 μM). 24 hours post transfection, culture
715 media was removed and replaced with fresh medium containing either Choloroquine or MG 132
716 as indicated. Arrow indicates HIF1α band. (E) Lysosomal translocation of HIF1α by KSHV-
717 encoded vCyclin. GFP signals represents expressed vCyclin. Lysosomes were stained with

718 lysotracker red. HIF1α was probed with Alexa 350 (blue). Arrow indicates representative HIF1α
719 localization.

720 **Fig. 5:** ChIP sequencing for HIF1α enrichment on KSHV genome in infected PBMCs or BC3
721 cells grown under normoxic or hypoxic conditions. (A) KSHV infection of PBMCs. BC3 cells
722 were used to reactivate KSHV by TPA/BA treatment. A multiplicity of infection equal to 10 was
723 used for infecting PBMCs in the presence of 20 µg/ml polybrene for 4 hours followed by
724 changing infection medium to fresh medium without polybrene and grown for another 24 hours.
725 Cells were divided into two halves and grown either under normoxic or hypoxic conditions for
726 24 hours. A small fraction of cells were taken out to check the infection by LANA immuno-
727 fluorescence. The bar diagram represents the infection rate. (B) Western blot analysis of LANA
728 in mock or KSHV infected cells grown under normoxic or hypoxic conditions. GAPDH served
729 as the loading control. (C) Western blot analysis of LANA in KSHV positive BC3 cells grown
730 under normoxic or hypoxic conditions. (D and E) Alignment of ChIP sequencing reads with
731 KSHV genome in infected PBMCs and KSHV-positive BC3 cells grown under normoxic or
732 hypoxic conditions. The ChIP sequencing data was analyzed using CLCbio software (Qiagen).
733 The highlighted sections represent regions with significant differential enrichment.

734

735 **Fig. 6:** vCyclin knock down KSHV-positive cells show compromised growth potential in
736 hypoxic conditions. (A) Generation of vCyclin knock down stable cells in KSHV positive BC3
737 cells. BC3 cells were transduced with ShvCyclin lentiviruses and selected in puromycin for 3
738 weeks. GFP positive cells represent successfully transduced stable cells. (B) Real-time PCR for
739 vCyclin in BC3 shControl and ShvCyclin stable cells (n=9; asterisk represents statistically
740 significant difference). (C) Relative copy number calculation of KSHV in BC3 shControl and

741 ShvCyclin stable cells grown under normoxic or hypoxic conditions. The experiments were
742 performed in triplicate. The error bar represents standard error from the mean. A p-value of
743 <0.05, was taken into consideration for statistical significance, (** p<0.001). (D) Representative
744 image for pulse field gel electrophoresis and Southern blot analysis for nucleotide analog pulsed
745 cells after proteinase K and Pme1 digestion. (E) Representative image for single molecule
746 analysis of replicated DNA of BC3 ShControl or BC3-ShvCyclin cells grown under hypoxic
747 conditions. Blue fluorescence represents KSHV specific probes; red represents incorporation of
748 IdU, while green represents CldU incorporation. (F) Bar digram for quantitation of replicated
749 KSHV molecules in BC3 ShControl or BC3-ShvCyclin cells grown under normoxic or hypoxic
750 conditions. (G) Colony focusing and soft agar assay to investigate *in-vitro* anchorage
751 dependent/independent grown potential of shControl and ShvCyclin of KSHV positive stable
752 cells grown under hypoxic conditions.
753
754 **Fig. 7:** Schematic for KSHV mediated attenuation of HIF1α mediated repression of DNA
755 replication in hypoxic conditions. A KSHV uninfected cell shows up-regulated expression of
756 HIF1α which restricts DNA replication in hypoxic conditions. In KSHV infected cells, KSHV-
757 encoded LANA and vGPCR promotes up-regulated expression of HIF1α through inhibiting its
758 proteosomal degradation or by working on MAPK/P38 pathway respectively. KSHV-encoded
759 vCyclin, which is also expressed in response to hypoxia, interacts and regulate HIF1α
760 transcriptional activity as well as degrade it through lysosomal pathway to balance HIF1α
761 mediated restriction of DNA replication in hypoxia.
762
763

764

765

766 **Supplementary Fig. 1:** (A) Representative image for LANA immuno-fluorescence in PBMCs
767 infected with mock or rKSHV. (B) Real-time PCR analysis for the transcriptional activity of
768 HIF1α by measuring expression of PDK1 in mock or rKSHV infected PBMCs grown under
769 normoxic or hypoxic conditions. The experiment was performed in triplicate (* $p<0.05$). (C)
770 Real-time PCR analysis for the transcriptional activity of HIF1α in HEK293T and HEK293T-
771 BAC16-KSHV cells grown under normoxic or hypoxic conditions. The cells were grown under
772 normoxic or hypoxic conditions followed by total RNA isolation and cDNA synthesis. Equal
773 amount of cDNA was used for expression analysis of HIF1α targets (LDHA, PDK1 and P4HA1)
774 by real-time PCR. The experiment was performed in triplicate. The error bar represents standard
775 error from the mean. A p-value of <0.05 (*) was taken into consideration for statistical
776 significance.

777

778 **Supplementary Fig. 2:** Real-time PCR expression analysis of HIF1α targets LDHA, P4HA1 and
779 PDK1 in HEK293T cells transfected with Mock, LANA, vGPCR, RTA, vCyclin or vFLIP
780 plasmids and grown under normoxic conditions. 48 hours post transfection, total RNA was
781 isolated from transfected cells followed by synthesis of cDNA using 2 µg of the total RNA. 1 µL
782 of 10 times diluted cDNA was used for quantitative real-time PCR. GAPDH was used as the
783 endogenous control. The experiments were done in triplicate. The error bar represents standard
784 error from the mean. A p-value of <0.05 (*) was taken into consideration for statistical
785 significance, (** $p<0.001$).

786

Supplementary Fig. 3: KSHV-encoded vCyclin showed gradual cytosolic translocation in transfected cells. HEK293T cells were transfectetd with mock or GFP-vCyclin encoding plasmids. 24 or 48 hours post transfection, cell were analyzed for cellular localization of expressed proteins through GFP fluorescence with respect to nucleus. The mock GFP showed an even distribution of GFP throughout the cells while vCyclin showed enhanced cytosolic localization at longer time points.

Supplementary Fig. 4: Dose dependent lysosomal degradation of HIF1α by KSHV-encoded vCyclin in Saos-2 Cells. (A) Microscopic visualization of vCyclin expression with increasing amounts of transfected plasmid. (B) HIF1α, GFP and GAPDH western blots in cells transfected with gradually increasing amounts of GFP-vCyclin. GFP western blot represents GFP-vCyclin. GAPDH was used as the loading control. Arrow indicates HIF1α band. (C) HIF1α western blot analysis of Saos-2 cells transfected with GFP-vCyclin and treated with increasing amounts of lysosomal inhibitor (Chloroquine; 0, 6.25, 12.5, 25 and 50μM).

Supplementary Fig. 5: HIF1α mediated up-regulation of vCyclin in KSHV positive BCBL1 and JSC1 cells. cells were grown under presence of $CoCl_2$ induced hypoxia followed by real-time PCR analysis (A) Confirmation for induction of hypoxia by HIF1α western blot. (B) Real-time PCR analysis for vCyclin expression in BCBL1 and JSC1 cells grown under normoxic or $CoCl_2$ induced hypoxia. (C) Schematic for hypoxia responsive elements (HREs) within the promoter of vCycin. (D) Luciferase assay for identification of HIF1α regulated HREs of vCyclin promoter.

809 **Table S1:** List of primers used to amplify various HREs constructs within vCyclin promoter and
810 for the real time PCR.

811 **Table S2:** HIF1α binding sites on KSHV genome in BC3 cells grown under hypoxic conditions.

812 **Table S3:** HIF1α binding sites on KSHV genome in BC3 cells grown under normoxic
813 conditions.

814 **Table S4:** HIF1α binding sites on KSHV genome in infected PBMCs grown under hypoxic
815 conditions.

816 **Table S5:** HIF1α binding sites on KSHV genome in infected PBMCs grown under normoxic
817 conditions.

818

819

References:

1. Boshoff C, Weiss R. AIDS-related malignancies. Nat Rev Cancer. 2002;2(5):373-82. doi: 10.1038/nrc797. PubMed PMID: 12044013.
2. Goncalves PH, Ziegelbauer J, Uldrick TS, Yarchoan R. Kaposi sarcoma herpesvirus-associated cancers and related diseases. Curr Opin HIV AIDS. 2017;12(1):47-56. Epub 2016/09/24. doi: 10.1097/COH.0000000000000330. PubMed PMID: 27662501.
3. Chang Y, Cesarman E, Pessin MS, Lee F, Culpepper J, Knowles DM, et al. Identification of herpesvirus-like DNA sequences in AIDS-associated Kaposi's sarcoma. Science. 1994;266(5192):1865-9. Epub 1994/12/16. PubMed PMID: 7997879.
4. Cantos VD, Kalapila AG, Ly Nguyen M, Adamski M, Gunthel CJ. Experience with Kaposi Sarcoma Herpesvirus Inflammatory Cytokine Syndrome in a Large Urban HIV Clinic in the United States: Case Series and Literature Review. Open Forum Infect Dis. 2017;4(4):ofx196. Epub 2018/05/17. doi: 10.1093/ofid/ofx196. PubMed PMID: 29766014; PubMed Central PMCID: PMC5946878.
5. Polizzotto MN, Uldrick TS, Hu D, Yarchoan R. Clinical Manifestations of Kaposi Sarcoma Herpesvirus Lytic Activation: Multicentric Castleman Disease (KSHV-MCD) and the KSHV Inflammatory Cytokine Syndrome. Front Microbiol. 2012;3:73. Epub 2012/03/10. doi: 10.3389/fmicb.2012.00073. PubMed PMID: 22403576; PubMed Central PMCID: PMC3291870.
6. Russo JJ, Bohenzky RA, Chien MC, Chen J, Yan M, Maddalena D, et al. Nucleotide sequence of the Kaposi sarcoma-associated herpesvirus (HHV8). Proc Natl Acad Sci U S A. 1996;93(25):14862-7. Epub 1996/12/10. PubMed PMID: 8962146; PubMed Central PMCID: PMC26227.
7. Mesri EA, Feitelson MA, Munger K. Human viral oncogenesis: a cancer hallmarks analysis. Cell Host Microbe. 2014;15(3):266-82. Epub 2014/03/19. doi: 10.1016/j.chom.2014.02.011. PubMed PMID: 24629334; PubMed Central PMCID: PMC3992243.
8. Giffin L, Damania B. KSHV: pathways to tumorigenesis and persistent infection. Adv Virus Res. 2014;88:111-59. Epub 2014/01/01. doi: 10.1016/B978-0-12-800098-4.00002-7. PubMed PMID: 24373311; PubMed Central PMCID: PMC4104069.
9. Chandran B. Early events in Kaposi's sarcoma-associated herpesvirus infection of target cells. J Virol. 2010;84(5):2188-99. doi: 10.1128/JVI.01334-09. PubMed PMID: 19923183; PubMed Central PMCID: PMCPMC2820927.
10. Nicol SM, Sabbah S, Brulois KF, Jung JU, Bell AI, Hislop AD. Primary B Lymphocytes Infected with Kaposi's Sarcoma-Associated Herpesvirus Can Be Expanded In Vitro and Are Recognized by LANA-Specific CD4+ T Cells. J Virol. 2016;90(8):3849-59. doi: 10.1128/JVI.02377-15. PubMed PMID: 26819313; PubMed Central PMCID: PMCPMC4810529.
11. Uppal T, Jha HC, Verma SC, Robertson ES. Chromatinization of the KSHV Genome During the KSHV Life Cycle. Cancers (Basel). 2015;7(1):112-42. Epub 2015/01/17. doi: 10.3390/cancers7010112. PubMed PMID: 25594667; PubMed Central PMCID: PMC4381254.
12. Toth Z, Maglinte DT, Lee SH, Lee HR, Wong LY, Brulois KF, et al. Epigenetic analysis of KSHV latent and lytic genomes. PLoS Pathog. 2010;6(7):e1001013. Epub 2010/07/28. doi: 10.1371/journal.ppat.1001013. PubMed PMID: 20661424; PubMed Central PMCID: PMC2908616.
13. Arias C, Weisburd B, Stern-Ginossar N, Mercier A, Madrid AS, Bellare P, et al. KSHV 2.0: a comprehensive annotation of the Kaposi's sarcoma-associated herpesvirus genome using next-generation sequencing reveals novel genomic and functional features. PLoS Pathog. 2014;10(1):e1003847. doi: 10.1371/journal.ppat.1003847. PubMed PMID: 24453964; PubMed Central PMCID: PMCPMC3894221.
14. Damania B. Oncogenic gamma-herpesviruses: comparison of viral proteins involved in tumorigenesis. Nat Rev Microbiol. 2004;2(8):656-68. doi: 10.1038/nrmicro958. PubMed PMID: 15263900.

15. Uppal T, Banerjee S, Sun Z, Verma SC, Robertson ES. KSHV LANA--the master regulator of KSHV latency. Viruses. 2014;6(12):4961-98. Epub 2014/12/17. doi: 10.3390/v6124961. PubMed PMID: 25514370; PubMed Central PMCID: PMC4276939.

16. Cotter MA, 2nd, Robertson ES. The latency-associated nuclear antigen tethers the Kaposi's sarcoma-associated herpesvirus genome to host chromosomes in body cavity-based lymphoma cells. Virology. 1999;264(2):254-64. doi: 10.1006/viro.1999.9999. PubMed PMID: 10562490.

17. Ballestas ME, Chatis PA, Kaye KM. Efficient persistence of extrachromosomal KSHV DNA mediated by latency-associated nuclear antigen. Science. 1999;284(5414):641-4. Epub 1999/04/24. PubMed PMID: 10213686.

18. Schwam DR, Luciano RL, Mahajan SS, Wong L, Wilson AC. Carboxy terminus of human herpesvirus 8 latency-associated nuclear antigen mediates dimerization, transcriptional repression, and targeting to nuclear bodies. J Virol. 2000;74(18):8532-40. Epub 2000/08/23. PubMed PMID: 10954554; PubMed Central PMCID: PMC116365.

19. Wei F, Gan J, Wang C, Zhu C, Cai Q. Cell Cycle Regulatory Functions of the KSHV Oncoprotein LANA. Front Microbiol. 2016;7:334. Epub 2016/04/12. doi: 10.3389/fmicb.2016.00334. PubMed PMID: 27065950; PubMed Central PMCID: PMC4811921.

20. Friborg J, Jr., Kong W, Hottiger MO, Nabel GJ. p53 inhibition by the LANA protein of KSHV protects against cell death. Nature. 1999;402(6764):889-94. Epub 2000/01/06. doi: 10.1038/47266. PubMed PMID: 10622254.

21. Gasperini P, Espigol-Frigole G, McCormick PJ, Salvucci O, Maric D, Uldrick TS, et al. Kaposi sarcoma herpesvirus promotes endothelial-to-mesenchymal transition through Notch-dependent signaling. Cancer Res. 2012;72(5):1157-69. Epub 2012/01/13. doi: 10.1158/0008-5472.CAN-11-3067. PubMed PMID: 22237624; PubMed Central PMCID: PMC3512101.

22. Jha HC, Sun Z, Upadhyay SK, El-Naccache DW, Singh RK, Sahu SK, et al. KSHV-Mediated Regulation of Par3 and SNAIL Contributes to B-Cell Proliferation. PLoS Pathog. 2016;12(7):e1005801. doi: 10.1371/journal.ppat.1005801. PubMed PMID: 27463802; PubMed Central PMCID: PMCPMC4963126.

23. Lang F, Sun Z, Pei Y, Singh RK, Jha HC, Robertson ES. Shugoshin 1 is dislocated by KSHV-encoded LANA inducing aneuploidy. PLoS Pathog. 2018;14(9):e1007253. doi: 10.1371/journal.ppat.1007253. PubMed PMID: 30212568; PubMed Central PMCID: PMCPMC6136811.

24. Jones T, Ramos da Silva S, Bedolla R, Ye F, Zhou F, Gao SJ. Viral cyclin promotes KSHV-induced cellular transformation and tumorigenesis by overriding contact inhibition. Cell Cycle. 2014;13(5):845-58. Epub 2014/01/15. doi: 10.4161/cc.27758. PubMed PMID: 24419204; PubMed Central PMCID: PMC3979920.

25. Verschuren EW, Klefstrom J, Evan GI, Jones N. The oncogenic potential of Kaposi's sarcoma-associated herpesvirus cyclin is exposed by p53 loss in vitro and in vivo. Cancer Cell. 2002;2(3):229-41. Epub 2002/09/21. PubMed PMID: 12242155.

26. Sun SC, Cesarman E. NF-kappaB as a target for oncogenic viruses. Curr Top Microbiol Immunol. 2011;349:197-244. Epub 2010/09/17. doi: 10.1007/82_2010_108. PubMed PMID: 20845110; PubMed Central PMCID: PMC3855473.

27. Zhao J, He S, Minassian A, Li J, Feng P. Recent advances on viral manipulation of NF-kappaB signaling pathway. Curr Opin Virol. 2015;15:103-11. Epub 2015/09/20. doi: 10.1016/j.coviro.2015.08.013. PubMed PMID: 26385424; PubMed Central PMCID: PMC4688235.

28. Rahman MM, McFadden G. Modulation of NF-kappaB signalling by microbial pathogens. Nat Rev Microbiol. 2011;9(4):291-306. Epub 2011/03/09. doi: 10.1038/nrmicro2539. PubMed PMID: 21383764; PubMed Central PMCID: PMC3611960.

29. Choi YB, Sandford G, Nicholas J. Human herpesvirus 8 interferon regulatory factor-mediated BH3-only protein inhibition via Bid BH3-B mimicry. PLoS Pathog. 2012;8(6):e1002748. Epub 2012/06/12. doi: 10.1371/journal.ppat.1002748. PubMed PMID: 22685405; PubMed Central PMCID: PMC3369933.

30. Montaner S, Kufareva I, Abagyan R, Gutkind JS. Molecular mechanisms deployed by virally encoded G protein-coupled receptors in human diseases. Annu Rev Pharmacol Toxicol. 2013;53:331-54. Epub 2012/10/25. doi: 10.1146/annurev-pharmtox-010510-100608. PubMed PMID: 23092247; PubMed Central PMCID: PMC4074518.

31. Vischer HF, Siderius M, Leurs R, Smit MJ. Herpesvirus-encoded GPCRs: neglected players in inflammatory and proliferative diseases? Nat Rev Drug Discov. 2014;13(2):123-39. Epub 2014/01/22. doi: 10.1038/nrd4189. PubMed PMID: 24445563.

32. Ye F, Lei X, Gao SJ. Mechanisms of Kaposi's Sarcoma-Associated Herpesvirus Latency and Reactivation. Adv Virol. 2011;2011. Epub 2011/06/01. doi: 10.1155/2011/193860. PubMed PMID: 21625290; PubMed Central PMCID: PMC3103228.

33. Aneja KK, Yuan Y. Reactivation and Lytic Replication of Kaposi's Sarcoma-Associated Herpesvirus: An Update. Front Microbiol. 2017;8:613. Epub 2017/05/06. doi: 10.3389/fmicb.2017.00613. PubMed PMID: 28473805; PubMed Central PMCID: PMC5397509.

34. Davis DA, Rinderknecht AS, Zoeteweij JP, Aoki Y, Read-Connole EL, Tosato G, et al. Hypoxia induces lytic replication of Kaposi sarcoma-associated herpesvirus. Blood. 2001;97(10):3244-50. doi: 10.1182/blood.v97.10.3244. PubMed PMID: 11342455.

35. Cai Q, Lan K, Verma SC, Si H, Lin D, Robertson ES. Kaposi's sarcoma-associated herpesvirus latent protein LANA interacts with HIF-1 alpha to upregulate RTA expression during hypoxia: Latency control under low oxygen conditions. J Virol. 2006;80(16):7965-75. doi: 10.1128/JVI.00689-06. PubMed PMID: 16873253; PubMed Central PMCID: PMCPMC1563785.

36. Ye F, Zhou F, Bedolla RG, Jones T, Lei X, Kang T, et al. Reactive oxygen species hydrogen peroxide mediates Kaposi's sarcoma-associated herpesvirus reactivation from latency. PLoS Pathog. 2011;7(5):e1002054. Epub 2011/06/01. doi: 10.1371/journal.ppat.1002054. PubMed PMID: 21625536; PubMed Central PMCID: PMC3098240.

37. Mason EF, Rathmell JC. Cell metabolism: an essential link between cell growth and apoptosis. Biochim Biophys Acta. 2011;1813(4):645-54. Epub 2010/09/08. doi: 10.1016/j.bbamcr.2010.08.011. PubMed PMID: 20816705; PubMed Central PMCID: PMC3010257.

38. Michiels C. Physiological and pathological responses to hypoxia. Am J Pathol. 2004;164(6):1875-82. Epub 2004/05/27. doi: 10.1016/S0002-9440(10)63747-9. PubMed PMID: 15161623; PubMed Central PMCID: PMC1615763.

39. Dengler VL, Galbraith M, Espinosa JM. Transcriptional regulation by hypoxia inducible factors. Crit Rev Biochem Mol Biol. 2014;49(1):1-15. doi: 10.3109/10409238.2013.838205. PubMed PMID: 24099156; PubMed Central PMCID: PMCPMC4342852.

40. Majmundar AJ, Wong WJ, Simon MC. Hypoxia-inducible factors and the response to hypoxic stress. Mol Cell. 2010;40(2):294-309. doi: 10.1016/j.molcel.2010.09.022. PubMed PMID: 20965423; PubMed Central PMCID: PMCPMC3143508.

41. Gardner LB, Li Q, Park MS, Flanagan WM, Semenza GL, Dang CV. Hypoxia inhibits G1/S transition through regulation of p27 expression. J Biol Chem. 2001;276(11):7919-26. Epub 2000/12/12. doi: 10.1074/jbc.M010189200. PubMed PMID: 11112789.

42. Hammond EM, Denko NC, Dorie MJ, Abraham RT, Giaccia AJ. Hypoxia links ATR and p53 through replication arrest. Mol Cell Biol. 2002;22(6):1834-43. Epub 2002/02/28. PubMed PMID: 11865061; PubMed Central PMCID: PMC135616.

43. Goda N, Ryan HE, Khadivi B, McNulty W, Rickert RC, Johnson RS. Hypoxia-inducible factor 1alpha is essential for cell cycle arrest during hypoxia. Mol Cell Biol. 2003;23(1):359-69. PubMed PMID: 12482987; PubMed Central PMCID: PMCPMC140666.

44. Cuninghame S, Jackson R, Zehbe I. Hypoxia-inducible factor 1 and its role in viral carcinogenesis. Virology. 2014;456-457:370-83. Epub 2014/04/05. doi: 10.1016/j.virol.2014.02.027. PubMed PMID: 24698149.

963 45. Singh RK, Lang F, Pei Y, Jha HC, Robertson ES. Metabolic reprogramming of Kaposi's sarcoma
964 associated herpes virus infected B-cells in hypoxia. PLoS Pathog. 2018;14(5):e1007062. doi:
965 10.1371/journal.ppat.1007062. PubMed PMID: 29746587; PubMed Central PMCID: PMCPMC5963815.
966 46. Veeranna RP, Haque M, Davis DA, Yang M, Yarchoan R. Kaposi's sarcoma-associated herpesvirus
967 latency-associated nuclear antigen induction by hypoxia and hypoxia-inducible factors. J Virol.
968 2012;86(2):1097-108. doi: 10.1128/JVI.05167-11. PubMed PMID: 22090111; PubMed Central PMCID:
969 PMCPMC3255810.
970 47. Hayashi M, Saito Y, Kawashima S. Calpain activation is essential for membrane fusion of
971 erythrocytes in the presence of exogenous Ca2+. Biochem Biophys Res Commun. 1992;182(2):939-46.
972 PubMed PMID: 1734892.
973 48. Yuan Y, Hilliard G, Ferguson T, Millhorn DE. Cobalt inhibits the interaction between hypoxia-
974 inducible factor-alpha and von Hippel-Lindau protein by direct binding to hypoxia-inducible factor-alpha.
975 J Biol Chem. 2003;278(18):15911-6. doi: 10.1074/jbc.M300463200. PubMed PMID: 12606543.
976 49. Hubbi ME, Kshitiz, Gilkes DM, Rey S, Wong CC, Luo W, et al. A nontranscriptional role for HIF-
977 1alpha as a direct inhibitor of DNA replication. Sci Signal. 2013;6(262):ra10. Epub 2013/02/14. doi:
978 10.1126/scisignal.2003417. PubMed PMID: 23405012; PubMed Central PMCID: PMC4124626.
979 50. Lin CL, Li H, Wang Y, Zhu FX, Kudchodkar S, Yuan Y. Kaposi's sarcoma-associated herpesvirus lytic
980 origin (ori-Lyt)-dependent DNA replication: identification of the ori-Lyt and association of K8 bZip
981 protein with the origin. J Virol. 2003;77(10):5578-88. PubMed PMID: 12719550; PubMed Central PMCID:
982 PMCPMC154033.
983 51. Verma SC, Lu J, Cai Q, Kosiyatrakul S, McDowell ME, Schildkraut CL, et al. Single molecule
984 analysis of replicated DNA reveals the usage of multiple KSHV genome regions for latent replication.
985 PLoS Pathog. 2011;7(11):e1002365. doi: 10.1371/journal.ppat.1002365. PubMed PMID: 22072974;
986 PubMed Central PMCID: PMCPMC3207954.
987 52. Seyfried TN, Shelton LM. Cancer as a metabolic disease. Nutr Metab (Lond). 2010;7:7. doi:
988 10.1186/1743-7075-7-7. PubMed PMID: 20181022; PubMed Central PMCID: PMCPMC2845135.
989 53. Noch E, Khalili K. Oncogenic viruses and tumor glucose metabolism: like kids in a candy store.
990 Mol Cancer Ther. 2012;11(1):14-23. doi: 10.1158/1535-7163.MCT-11-0517. PubMed PMID: 22234809;
991 PubMed Central PMCID: PMCPMC3257817.
992 54. Raz S, Sheban D, Gonen N, Stark M, Berman B, Assaraf YG. Severe hypoxia induces complete
993 antifolate resistance in carcinoma cells due to cell cycle arrest. Cell Death Dis. 2014;5:e1067. Epub
994 2014/02/22. doi: 10.1038/cddis.2014.39. PubMed PMID: 24556682; PubMed Central PMCID:
995 PMC3944254.
996 55. Ortiz-Barahona A, Villar D, Pescador N, Amigo J, del Peso L. Genome-wide identification of
997 hypoxia-inducible factor binding sites and target genes by a probabilistic model integrating
998 transcription-profiling data and in silico binding site prediction. Nucleic Acids Res. 2010;38(7):2332-45.
999 doi: 10.1093/nar/gkp1205. PubMed PMID: 20061373; PubMed Central PMCID: PMCPMC2853119.
1000 56. Bardos JI, Ashcroft M. Hypoxia-inducible factor-1 and oncogenic signalling. Bioessays.
1001 2004;26(3):262-9. doi: 10.1002/bies.20002. PubMed PMID: 14988927.
1002 57. Hubbi ME, Gilkes DM, Hu H, Kshitiz, Ahmed I, Semenza GL. Cyclin-dependent kinases regulate
1003 lysosomal degradation of hypoxia-inducible factor 1alpha to promote cell-cycle progression. Proc Natl
1004 Acad Sci U S A. 2014;111(32):E3325-34. Epub 2014/07/30. doi: 10.1073/pnas.1412840111. PubMed
1005 PMID: 25071185; PubMed Central PMCID: PMC4136593.
1006 58. Tanimoto K, Makino Y, Pereira T, Poellinger L. Mechanism of regulation of the hypoxia-inducible
1007 factor-1 alpha by the von Hippel-Lindau tumor suppressor protein. EMBO J. 2000;19(16):4298-309. Epub
1008 2000/08/16. doi: 10.1093/emboj/19.16.4298. PubMed PMID: 10944113; PubMed Central PMCID:
1009 PMC302039.

59. Pugh CW, Ratcliffe PJ. The von Hippel-Lindau tumor suppressor, hypoxia-inducible factor-1 (HIF-1) degradation, and cancer pathogenesis. Semin Cancer Biol. 2003;13(1):83-9. Epub 2003/01/01. PubMed PMID: 12507560.

60. Zinkernagel AS, Johnson RS, Nizet V. Hypoxia inducible factor (HIF) function in innate immunity and infection. J Mol Med (Berl). 2007;85(12):1339-46. Epub 2007/11/22. doi: 10.1007/s00109-007-0282-2. PubMed PMID: 18030436.

61. Semenza GL. Hypoxia-inducible factors: mediators of cancer progression and targets for cancer therapy. Trends Pharmacol Sci. 2012;33(4):207-14. Epub 2012/03/09. doi: 10.1016/j.tips.2012.01.005. PubMed PMID: 22398146; PubMed Central PMCID: PMC3437546.

62. Carroll PA, Kenerson HL, Yeung RS, Lagunoff M. Latent Kaposi's sarcoma-associated herpesvirus infection of endothelial cells activates hypoxia-induced factors. J Virol. 2006;80(21):10802-12. Epub 2006/09/08. doi: 10.1128/JVI.00673-06. PubMed PMID: 16956952; PubMed Central PMCID: PMC1641760.

63. Catrina SB, Botusan IR, Rantanen A, Catrina AI, Pyakurel P, Savu O, et al. Hypoxia-inducible factor-1alpha and hypoxia-inducible factor-2alpha are expressed in kaposi sarcoma and modulated by insulin-like growth factor-I. Clin Cancer Res. 2006;12(15):4506-14. Epub 2006/08/11. doi: 10.1158/1078-0432.CCR-05-2473. PubMed PMID: 16899596.

64. Ma T, Patel H, Babapoor-Farrokhran S, Franklin R, Semenza GL, Sodhi A, et al. KSHV induces aerobic glycolysis and angiogenesis through HIF-1-dependent upregulation of pyruvate kinase 2 in Kaposi's sarcoma. Angiogenesis. 2015;18(4):477-88. Epub 2015/06/21. doi: 10.1007/s10456-015-9475-4. PubMed PMID: 26092770; PubMed Central PMCID: PMC4659376.

65. Jham BC, Montaner S. The Kaposi's sarcoma-associated herpesvirus G protein-coupled receptor: Lessons on dysregulated angiogenesis from a viral oncogene. J Cell Biochem. 2010;110(1):1-9. Epub 2010/03/10. doi: 10.1002/jcb.22524. PubMed PMID: 20213674; PubMed Central PMCID: PMC3733450.

66. Jham BC, Ma T, Hu J, Chaisuparat R, Friedman ER, Pandolfi PP, et al. Amplification of the angiogenic signal through the activation of the TSC/mTOR/HIF axis by the KSHV vGPCR in Kaposi's sarcoma. PLoS One. 2011;6(4):e19103. Epub 2011/05/12. doi: 10.1371/journal.pone.0019103. PubMed PMID: 21559457; PubMed Central PMCID: PMC3084756.

67. Semenza GL. HIF-1: upstream and downstream of cancer metabolism. Curr Opin Genet Dev. 2010;20(1):51-6. Epub 2009/11/28. doi: 10.1016/j.gde.2009.10.009. PubMed PMID: 19942427; PubMed Central PMCID: PMC2822127.

68. Delgado T, Carroll PA, Punjabi AS, Margineantu D, Hockenbery DM, Lagunoff M. Induction of the Warburg effect by Kaposi's sarcoma herpesvirus is required for the maintenance of latently infected endothelial cells. Proc Natl Acad Sci U S A. 2010;107(23):10696-701. Epub 2010/05/26. doi: 10.1073/pnas.1004882107. PubMed PMID: 20498071; PubMed Central PMCID: PMC2890792.

69. Cai QL, Knight JS, Verma SC, Zald P, Robertson ES. EC5S ubiquitin complex is recruited by KSHV latent antigen LANA for degradation of the VHL and p53 tumor suppressors. PLoS Pathog. 2006;2(10):e116. Epub 2006/10/31. doi: 10.1371/journal.ppat.0020116. PubMed PMID: 17069461; PubMed Central PMCID: PMC1626105.

70. Sodhi A, Montaner S, Patel V, Zohar M, Bais C, Mesri EA, et al. The Kaposi's sarcoma-associated herpes virus G protein-coupled receptor up-regulates vascular endothelial growth factor expression and secretion through mitogen-activated protein kinase and p38 pathways acting on hypoxia-inducible factor 1alpha. Cancer Res. 2000;60(17):4873-80. Epub 2000/09/15. PubMed PMID: 10987301.

71. Shrestha P, Davis DA, Veeranna RP, Carey RF, Viollet C, Yarchoan R. Hypoxia-inducible factor-1 alpha as a therapeutic target for primary effusion lymphoma. PLoS Pathog. 2017;13(9):e1006628. Epub 2017/09/19. doi: 10.1371/journal.ppat.1006628. PubMed PMID: 28922425; PubMed Central PMCID: PMC5619862.

72. Box AH, Demetrick DJ. Cell cycle kinase inhibitor expression and hypoxia-induced cell cycle arrest in human cancer cell lines. Carcinogenesis. 2004;25(12):2325-35. Epub 2004/09/07. doi: 10.1093/carcin/bgh274. PubMed PMID: 15347600.

73. Green SL, Freiberg RA, Giaccia AJ. p21(Cip1) and p27(Kip1) regulate cell cycle reentry after hypoxic stress but are not necessary for hypoxia-induced arrest. Mol Cell Biol. 2001;21(4):1196-206. Epub 2001/02/07. doi: 10.1128/MCB.21.4.1196-1206.2001. PubMed PMID: 11158306; PubMed Central PMCID: PMC99573.

74. Martin L, Rainey M, Santocanale C, Gardner LB. Hypoxic activation of ATR and the suppression of the initiation of DNA replication through cdc6 degradation. Oncogene. 2012;31(36):4076-84. Epub 2011/12/20. doi: 10.1038/onc.2011.585. PubMed PMID: 22179839; PubMed Central PMCID: PMC3310967.

75. Chen L, Lagunoff M. Establishment and maintenance of Kaposi's sarcoma-associated herpesvirus latency in B cells. J Virol. 2005;79(22):14383-91. Epub 2005/10/29. doi: 10.1128/JVI.79.22.14383-14391.2005. PubMed PMID: 16254372; PubMed Central PMCID: PMC1280215.

76. Rossi T, Coppi A, Bruni E, Ruberto A, Santachiara S, Baggio G. Effects of anti-malarial drugs on MCF-7 and Vero cell replication. Anticancer Res. 2007;27(4B):2555-9. PubMed PMID: 17695553.

77. Han YH, Moon HJ, You BR, Park WH. The effect of MG132, a proteasome inhibitor on HeLa cells in relation to cell growth, reactive oxygen species and GSH. Oncol Rep. 2009;22(1):215-21. PubMed PMID: 19513526.

Fig. 1

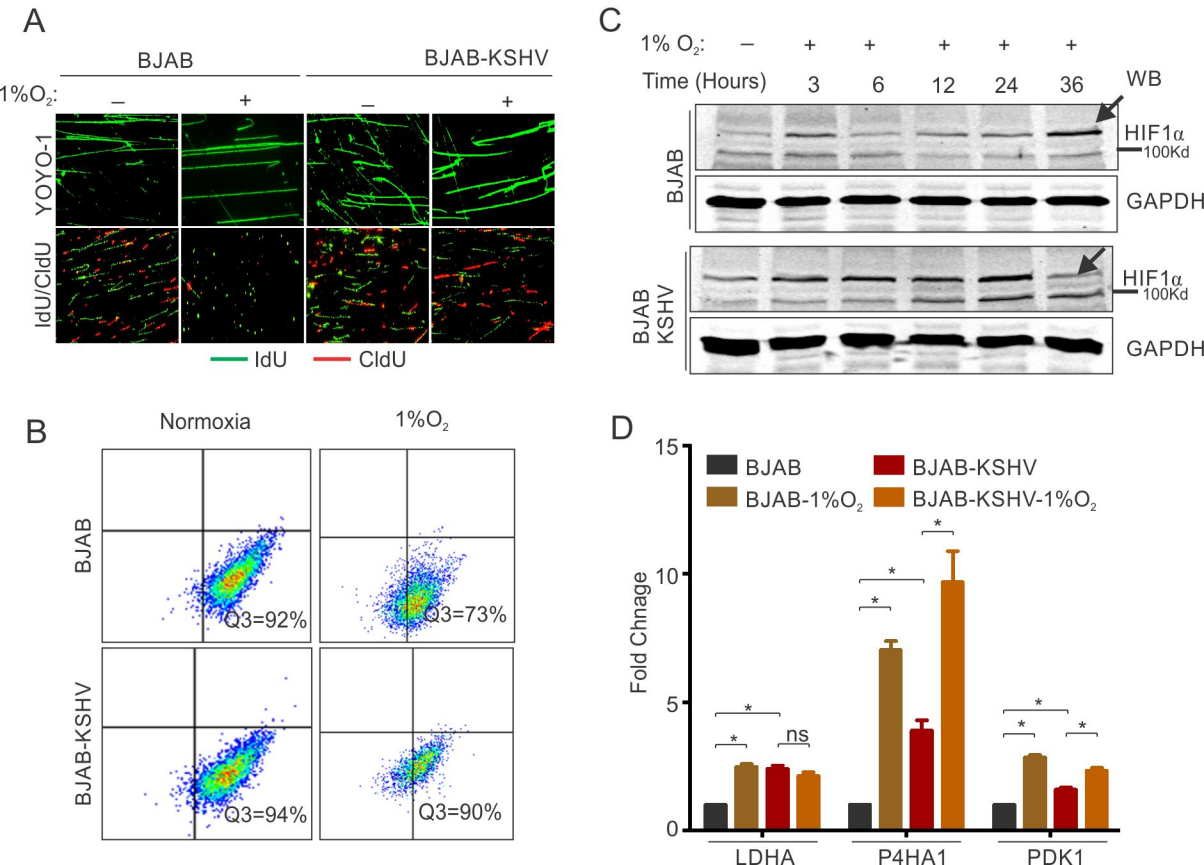
A
BJAB
BJAB-KSHV
1%O2:
–
+
–
+
YOYO-1
IdU/CldU
IdU
CldU
B
Normoxia
1%O2
BJAB
BJAB-KSHV
Q3=92%
Q3=73%
Q3=94%
Q3=90%
C
1% O2:
–
+
+
+
+
+
Time (Hours)
3
6
12
24
36
WB
BJAB
HIF1α
100Kd
GAPDH
BJAB KSHV
HIF1α
100Kd
GAPDH
D
Fold Chnage
15
10
5
0
BJAB
BJAB-KSHV
BJAB-1%O2
BJAB-KSHV-1%O2
ns
LDHA
P4HA1
PDK1

Fig. 2

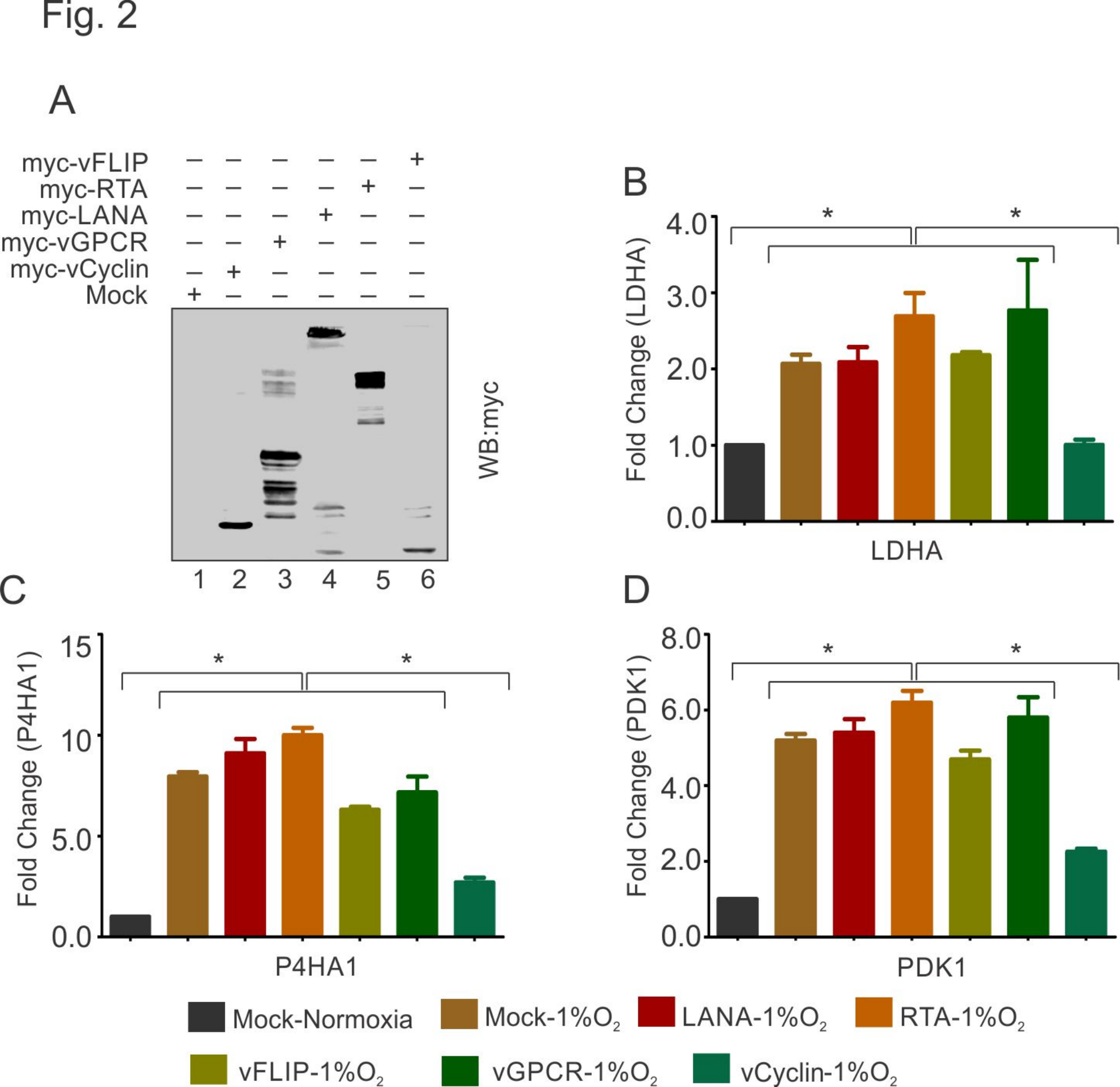
A
myc-vFLIP
myc-RTA
myc-LANA
myc-vGPCR
myc-vCyclin
Mock
WB:myc
1 2 3 4 5 6
B
Fold Change (LDHA)
LDHA
C
Fold Change (P4HA1)
P4HA1
D
Fold Change (PDK1)
PDK1
Mock-Normoxia
Mock-1%O2
LANA-1%O2
RTA-1%O2
vFLIP-1%O2
vGPCR-1%O2
vCyclin-1%O2

Fig. 3

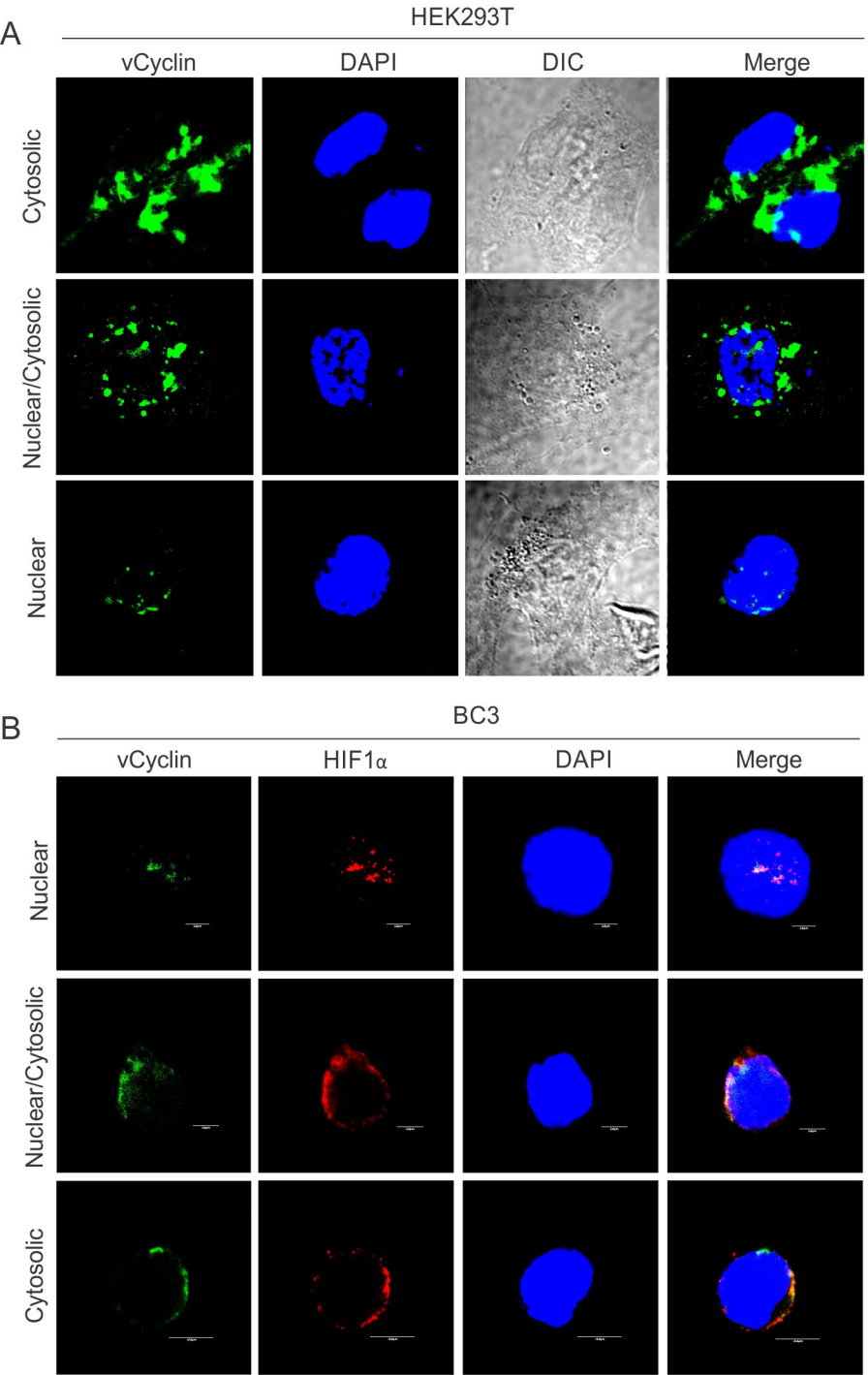
A
HEK293T
vCyclin
DAPI
DIC
Merge
Cytosolic
Nuclear/Cytosolic
Nuclear
B
BC3
vCyclin
HIF1α
DAPI
Merge
Nuclear
Nuclear/Cytosolic
Cytosolic

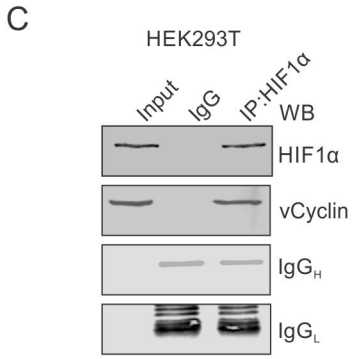
C
HEK293T
Input
IgG
IP:HIF1α
WB
HIF1α
vCyclin
IgG_H
IgG_L

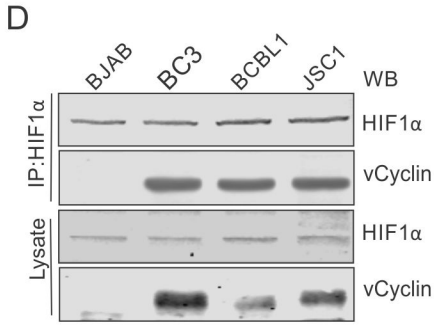
D
BJAB
BC3
BCBL1
JSC1
WB
IP:HIF1α
HIF1α
vCyclin
Lysate
HIF1α
vCyclin

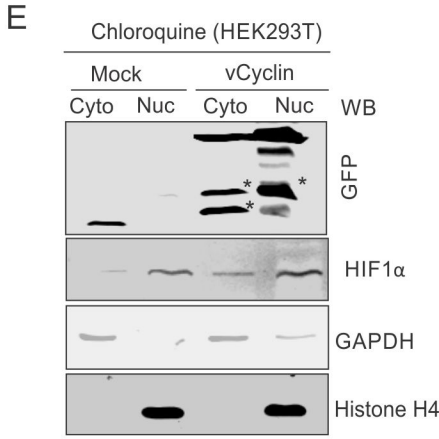
E
Chloroquine (HEK293T)
Mock
vCyclin
Cyto
Nuc
Cyto
Nuc
WB
GFP
HIF1α
GAPDH
Histone H4

Fig. 4

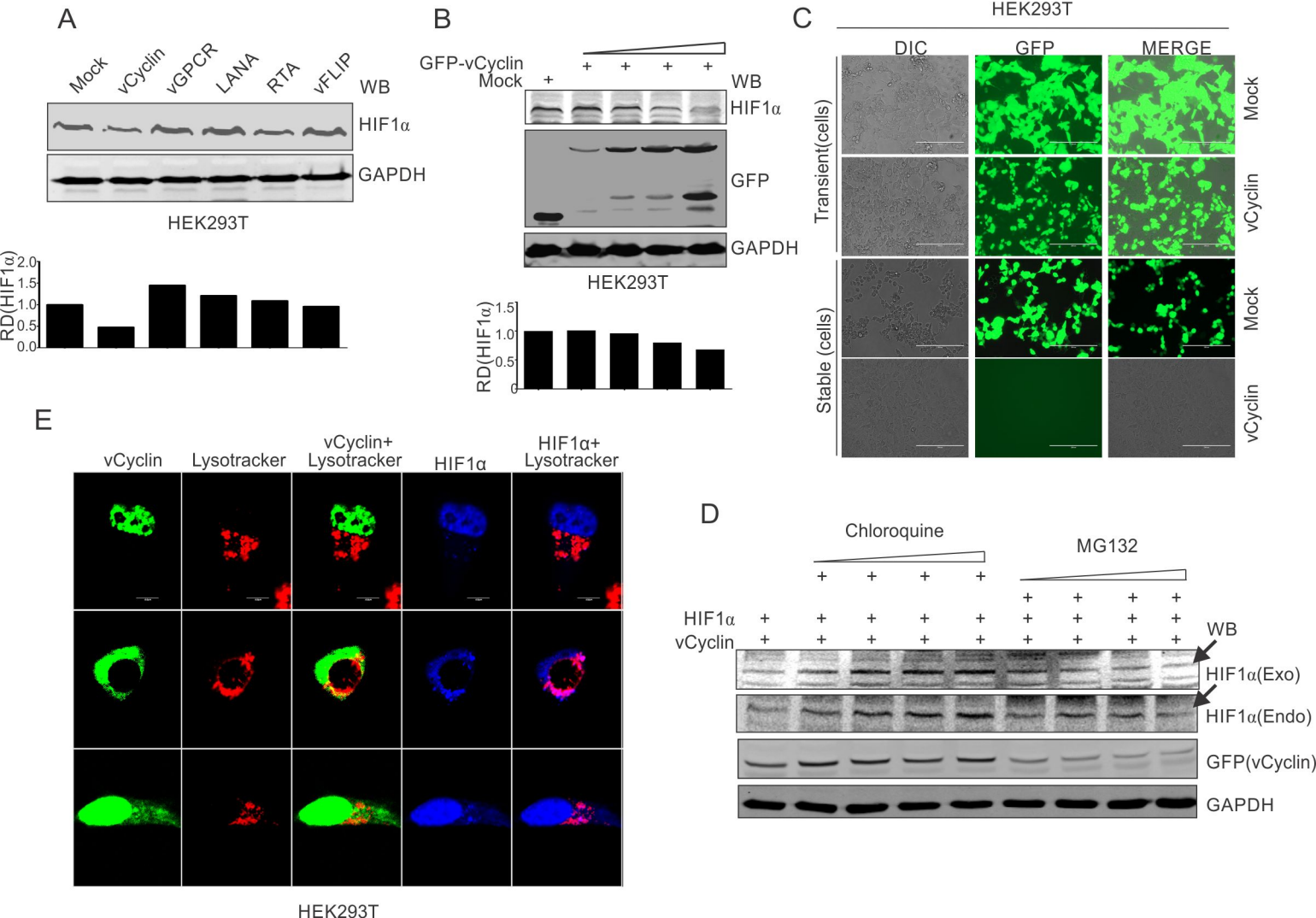
A
Mock
vCyclin
vGPCR
LANA
RTA
vFLIP
WB
HIF1α
GAPDH
HEK293T
RD(HIF1α)
2.0
1.5
1.0
0.5
0.0
B
GFP-vCyclin
Mock
+
WB
HIF1α
GFP
GAPDH
HEK293T
RD(HIF1α)
1.5
1.0
0.5
0
C
HEK293T
DIC
GFP
MERGE
Transient(cells)
Stable (cells)
Mock
vCyclin
Mock
vCyclin
E
vCyclin
Lysotracker
vCyclin+
Lysotracker
HIF1α
HIF1α+
Lysotracker
HEK293T
D
Chloroquine
MG132
HIF1α
vCyclin
WB
HIF1α(Exo)
HIF1α(Endo)
GFP(vCyclin)
GAPDH

Fig. 5

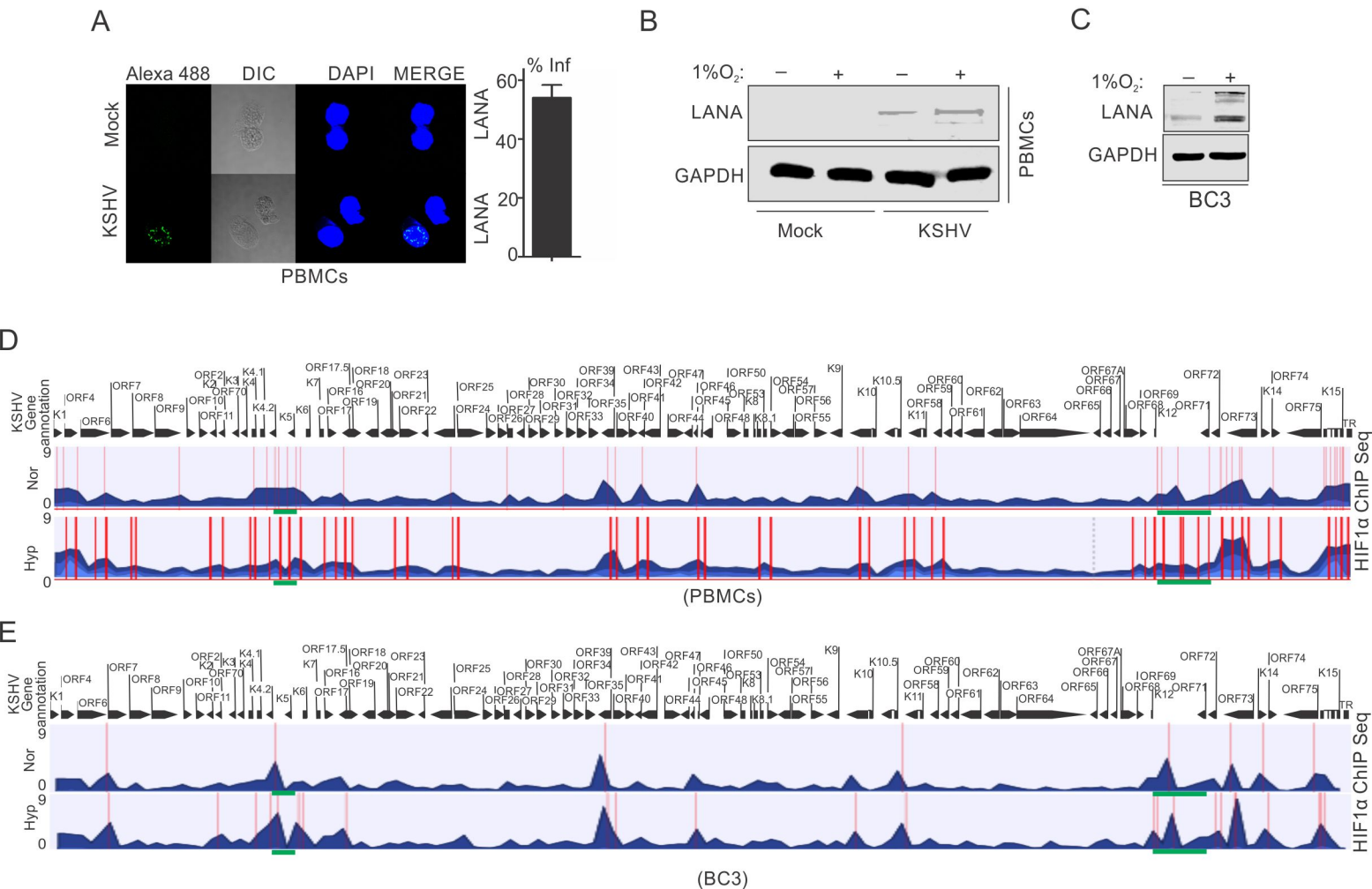
A
Alexa 488
DIC
DAPI
MERGE
Mock
KSHV
% Inf
LANA
LANA
PBMCs
B
1%O2:
LANA
GAPDH
PBMCs
Mock
KSHV
C
1%O2:
LANA
GAPDH
BC3
D
KSHV Gene annotation
Nor
Hyp
HIF1α ChIP Seq
(PBMCs)
E
KSHV Gene annotation
Nor
Hyp
HIF1α ChIP Seq
(BC3)

Fig. 6

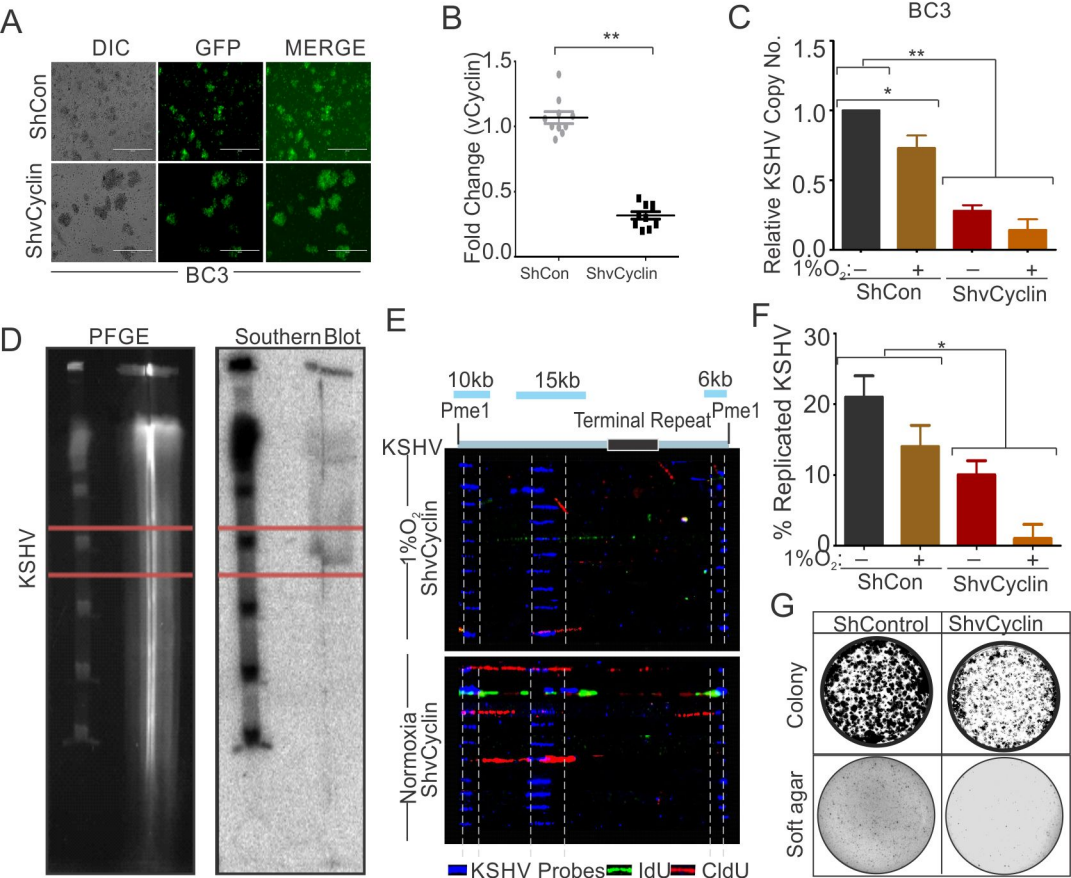
A
DIC
GFP
MERGE
ShCon
ShvCyclin
BC3
B
Fold Change (vCyclin)
**
ShCon
ShvCyclin
C
BC3
Relative KSHV Copy No.
**
*
1%O2:
ShCon
ShvCyclin
D
PFGE
Southern Blot
KSHV
E
10kb
15kb
6kb
Pme1
Terminal Repeat
Pme1
KSHV
1%O2 ShvCyclin
Normoxia ShvCyclin
KSHV Probes
IdU
CldU
F
% Replicated KSHV
*
1%O2:
ShCon
ShvCyclin
G
ShControl
ShvCyclin
Colony
Soft agar

Fig. 7

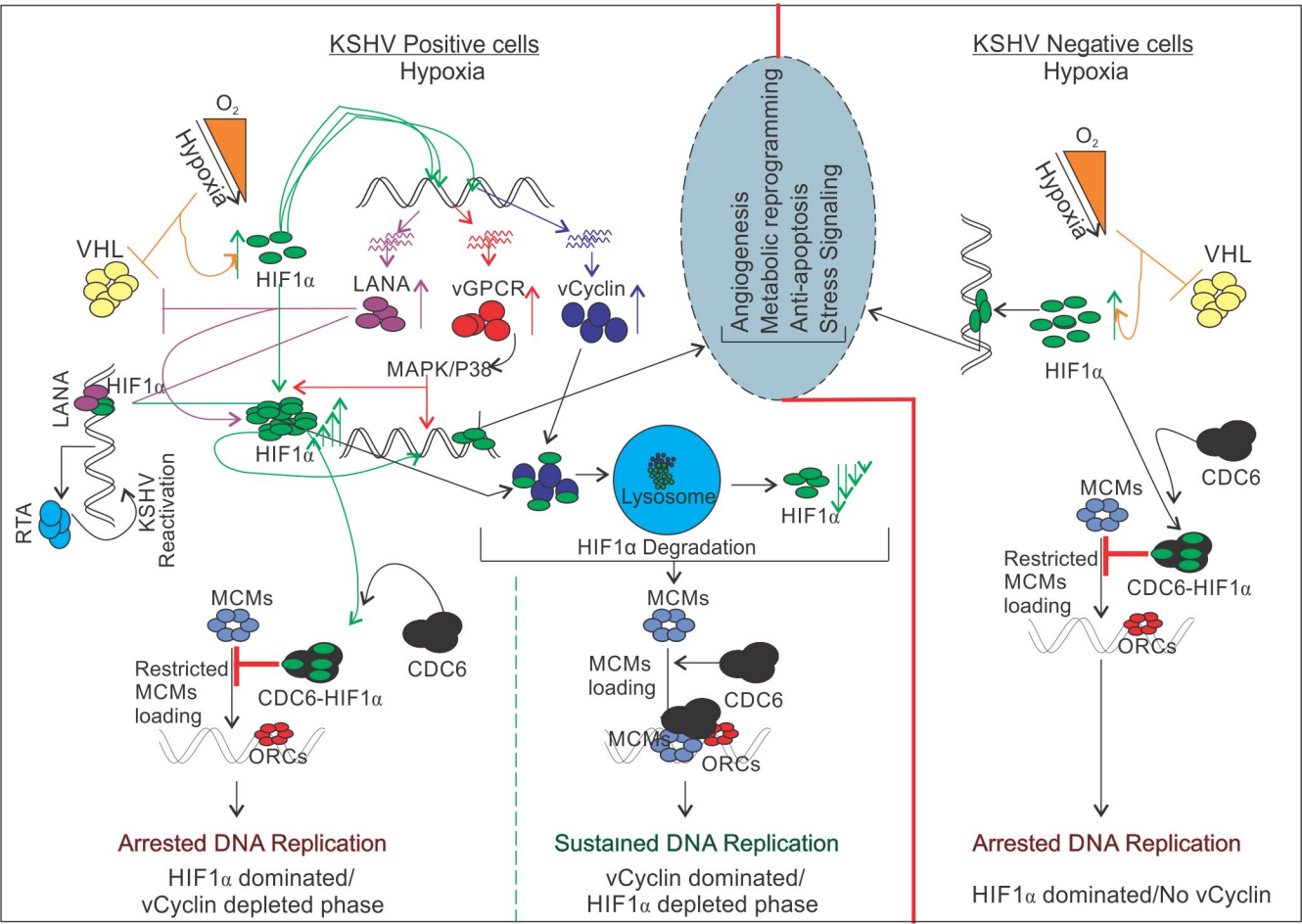
KSHV Positive cells
Hypoxia
KSHV Negative cells
Hypoxia
O2
Hypoxia
VHL
HIF1α
LANA
vGPCR
vCyclin
MAPK/P38
Angiogenesis
Metabolic reprogramming
Anti-apoptosis
Stress Signaling
RTA
KSHV Reactivation
Lysosome
HIF1α Degradation
MCMs
CDC6
Restricted MCMs loading
CDC6-HIF1α
ORCs
Arrested DNA Replication
HIF1α dominated/
vCyclin depleted phase
Sustained DNA Replication
vCyclin dominated/
HIF1α depleted phase
Arrested DNA Replication
HIF1α dominated/No vCyclin

Supplementary Figure 1

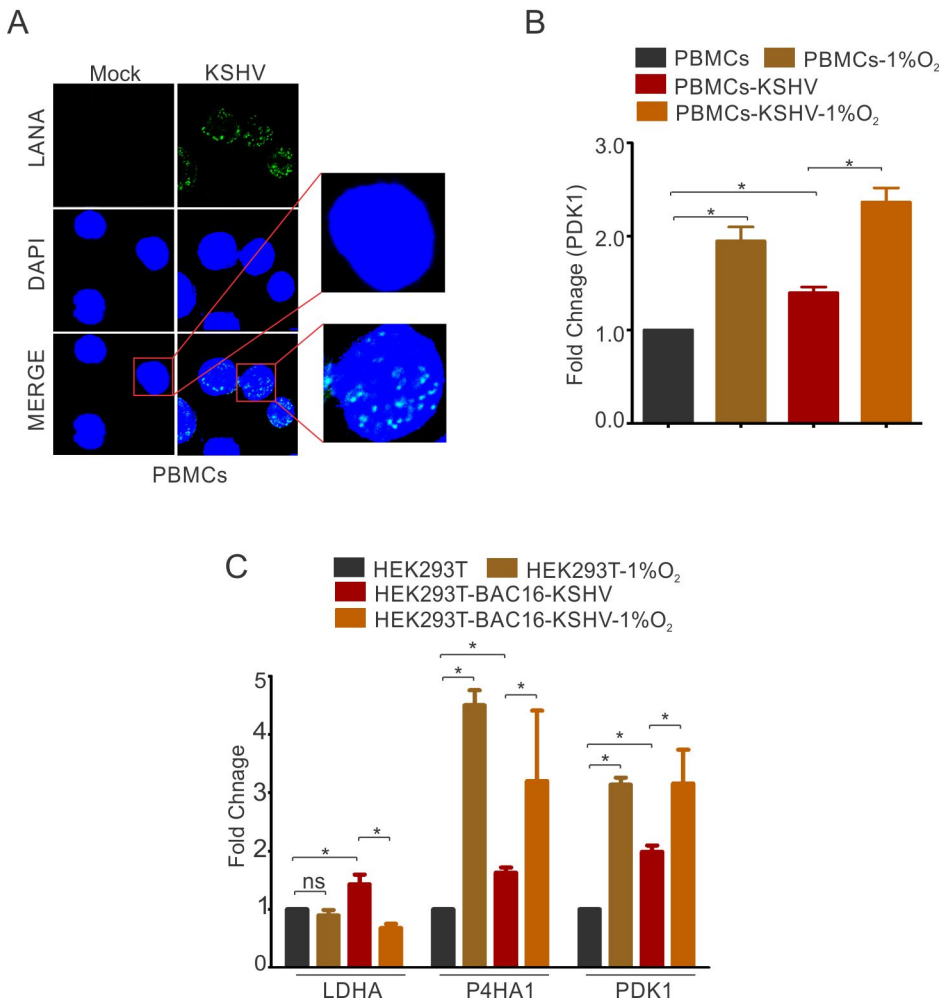

Supplementary Fig. 2

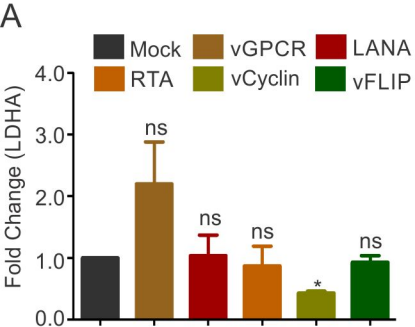

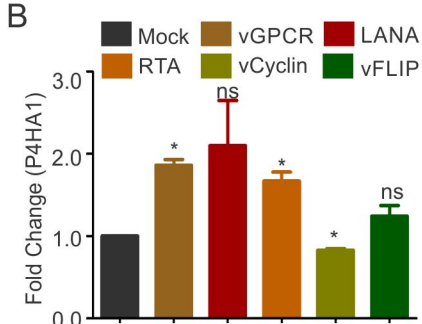

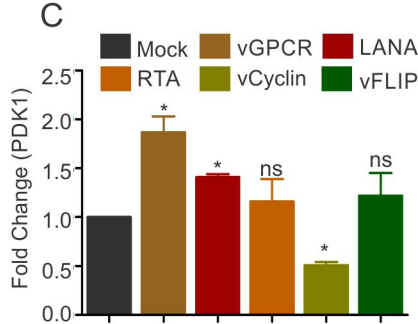

Supplementary Fig. 3

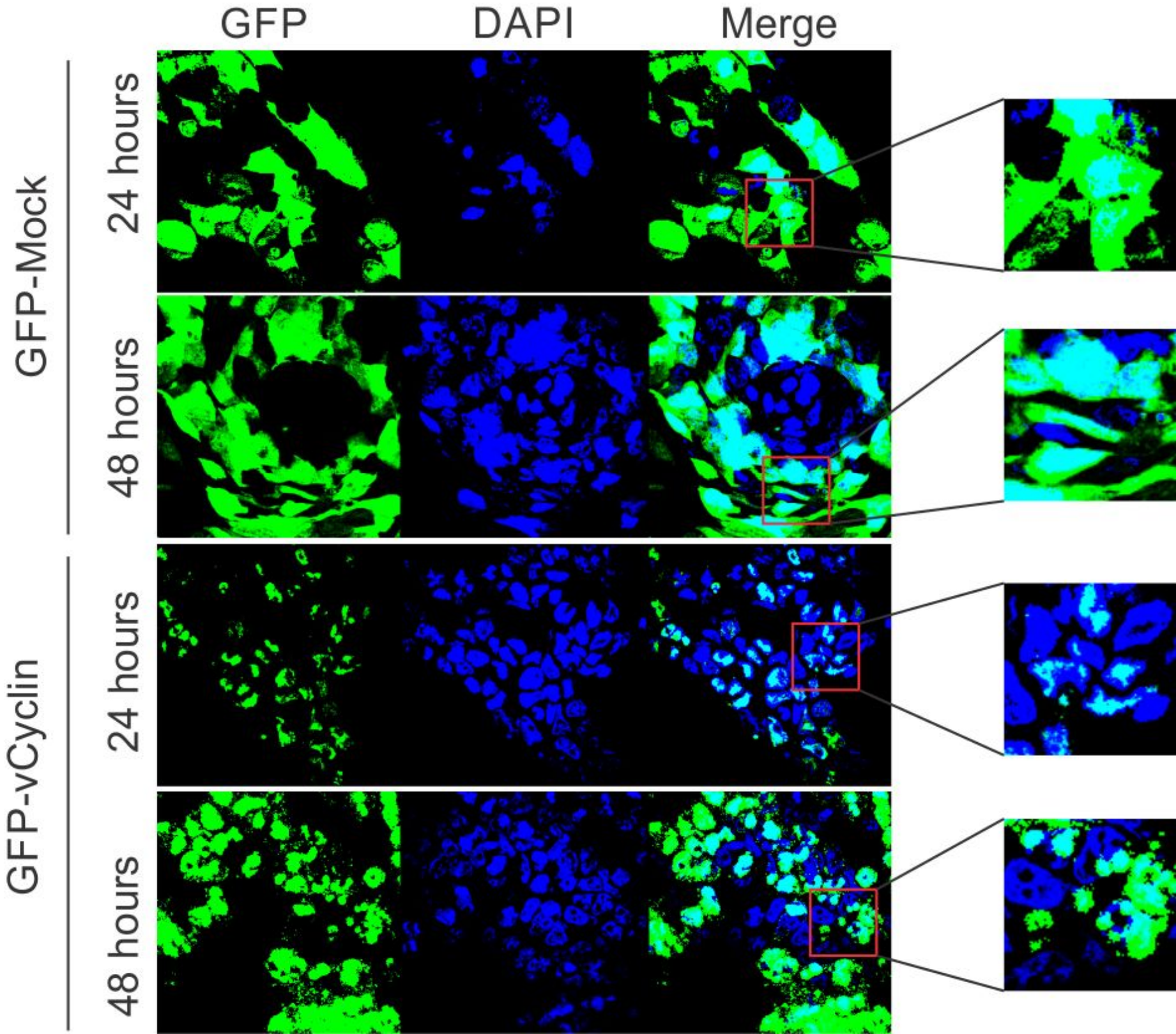

Supplementary Fig. 4

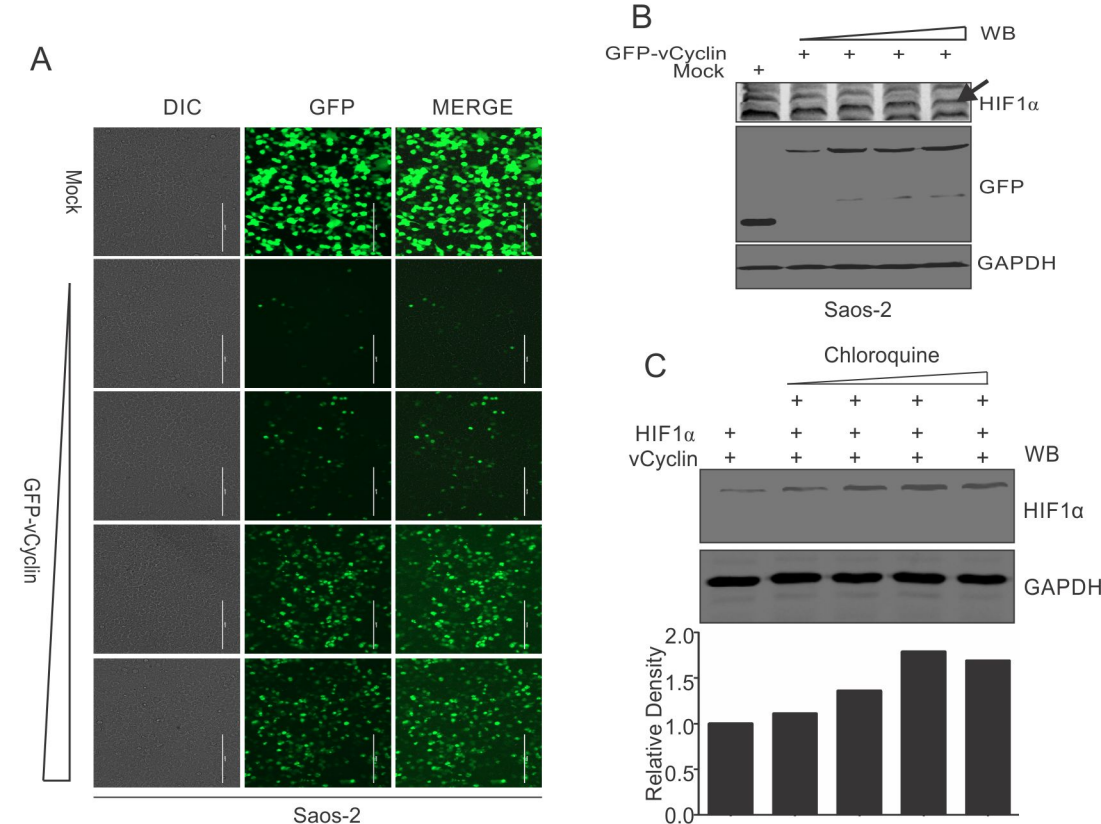

Supplementary Fig. 5